J. Plasma Physics (1998), *vol.* 60, *part* 3, *pp.* 627–671. Printed in the United Kingdom
© 1998 Cambridge University Press

Modelling RF heating in toroidal geometry: on the discrete bounce spectrum and the continuous bounce average

D. VAN EESTER

Laboratorium voor Plasmafysica/Laboratoire de Physique des Plasmas, Associatie 'Euratom–Belgische Staat'/Association 'Euratom–Etat Belge', Trilateral Euregio Cluster, Koninklijke Militaire School/Ecole Royale Militaire, Renaissancelaan 30, 1000 Brussels, Belgium

(Received 5 January 1998 and in revised form 10 March 1998)

Starting from a more general formalism due to Lamalle [*Plasma Phys. Contr. Fusion* **32**, 1409 (1997)], the dielectric response of a tokamak plasma to a radiofrequency (RF) perturbation is evaluated using a simple decorrelation model, assuming the poloidal cross-section of the magnetic surfaces to be circular and retaining leading-order terms in the drift parameter. Toroidicity, poloidal magnetic field and particle trapping are included in the model. Constants of the motion are used as independent variables. A semi-analytical method is adopted to evaluate the bounce spectrum of the dielectric response (needed to solve the wave equation) and the associated RF diffusion operator (required for solving the Fokker–Planck equation). The accent is on a study of this bounce spectrum. In particular, the link between the discrete bounce spectrum and the continuous bounce integral is highlighted. The critical parameter for the global justification of the replacement of the sum on the bounce spectrum by a bounce average is the relative magnitude of the decorrelation and bounce times. That for the local justification is the second derivative of the periodic part of the relative wave–particle phase. Numerical examples are provided to give a qualitative feeling for the justification of this substitution. The relation between the results presented here and those based on Hamiltonian models or on a simplified geometry is discussed.

1. Introduction and comments on the choice of independent variables

Over the last few years, much effort has been devoted to understanding the physics of heating of tokamak plasmas by electromagnetic waves in the radiofrequency (RF) range (see e.g. Jaeger *et al.* 1990, and references therein). Early modelling of this heating scheme, also referred to as ion cyclotron resonance heating (ICRH), was done assuming a magnetic field topology in which the field lines are straight. As a consequence of not treating the curvature of the magnetic field lines rigorously, a fundamental problem arose: although collisionless damping is not expected to be reversible in time when fields and particles are weakly decorrelated (e.g. by Coulomb collisions), early models could not guarantee positivity of the power absorption for energetic but Maxwellian particle populations in the weak-decorrelation limit. Lamalle (1993, 1994, 1997) explained this unphysical result as a consequence of the fact that

https://doi.org/10.1017/S0022377898007016 Published online by Cambridge University Press

expressions for the dielectric tensor obtained from straight-magnetic-field-line models were applied to toroidal plasmas in which the zeroth-order guiding-centre trajectories are *not* straight lines. He proposed a more rigorous approach based on the drift approximation, retaining up to first-order terms in the drift parameter. This approach is similar to the Hamiltonian action-angle formalism originally due to Kaufman (see e.g. Kaufman 1972; Gambier and Samain 1985; Bécoulet *et al*. 1991, 1994) and the gyrokinetic theory of Chen and Tsai (see e.g. Chen and Tsai 1983; Tsai *et al*. 1984). It relies on using the constants of the zeroth-order motion plus the time t_{gc} that the guiding centre needs to travel from the equatorial plane to a given poloidal position, the guiding centre's toroidal angle and finally the particle velocity's gyrophase ϕ as the independent variables. The obtained expressions clearly reveal the resonant character of the wave–particle interaction, and permit one to describe the fully non-local plasma response to an electromagnetic perturbation in toroidal geometry, including trapped-particle finite-banana-width effects. The work presented here adopts Lamalle's approach, but differs from it in two respects. First, only leading-order terms in the drift parameter ρ/L (where ρ is the Larmor radius and L the scale length on which the static magnetic field, density or temperature vary significantly) are retained, whereas Lamalle's work includes all terms up to first order in ρ/L. Although less general, the advantage of our approach is that the link with existing formulae in the literature is immediate. A second, minor, difference is that other independent variables are used. A first paper on the model adopted here was published in 1995 (Van Eester 1995). The present work adds a detailed discussion of the practical evaluation of various quantities, and provides a study on the justification of assumptions made to retrieve commonly used results.

From a practical point of view, adopting expressions such as the general formulae proposed by Lamalle is extremely challenging for current computers: since the complete bounce spectrum of the RF perturbation contains hundreds or thousands of modes, enormous amounts of computer time and memory storage are required to rigorously describe the interaction of the RF field with the particles. Lamalle explained that, in the limiting case where the bounce spectrum contains a very large number of modes, asymptotic techniques can be used and less general but less CPU-time-consuming expressions can be found. Louis examined the perspectives of Lamalle's model without sacrificing any of the details of the wave–particle crosstalk but assuming a circular plasma cross-section and neglecting drifts (Louis 1996, 1998; Louis and Lamalle 1996). One of his conclusions was that in a not-too-hot plasma, the partial absorbed power associated with a guiding-centre orbit scales with energy in exactly the way that simple resonance-crossing models predict. On the other hand, he showed that energetic tails and α particles (characterized by small collision frequencies and thus relatively long decorrelation times) require a more detailed description of the decorrelation. This was further confirmed in a study focusing on the effect of the role of the decorrelation (Van Eester *et al*. 1996). For sufficiently short decorrelation times (well below the bounce time), it was found that the details of the decorrelation model are irrelevant, implying that plasma models invoking an infinitely short decorrelation time can be used without sacrificing any physical details. The opposite limit of very long decorrelation times allows one to compute the dielectric response, *ignoring* the decorrelation effect as well.

https://doi.org/10.1017/S0022377898007016 Published online by Cambridge University Press

In this limit, decorrelation is only invoked to ensure causality. In practice, one replaces the real driver frequency ω by the complex frequency $\omega + i\nu$, where ν is commonly interpreted as the Coulomb collision frequency. Since the Coulomb collision frequency is finite but usually small compared with ω, one simply substitutes 0^+ for ν/ω when evaluating the dielectric response. Because the guiding-centre orbits are poloidally closed in a tokamak, a supplementary time scale is added to the RF heating problem when addressing it in toroidal geometry. A new subtlety involving the relative magnitude of the bounce and collision frequencies ω_b and ν then emerges: the decorrelation process, which is slow on the cyclotron time scale, can either be fast or slow on the bounce time scale. In the former case, where $\omega_b \ll \nu \ll \omega$ holds, it will be shown later that the expression obtained for the absorbed RF power is very similar to the usual quasi-uniform plasma expressions (e.g. the one that Stix (1975) obtains using a model with locally straight guiding-centre trajectories) and that the total absorbed power can be written either as a sum of the absorbed powers over individual poloidal bounce spectrum modes or as an equivalent bounce integral. In the case where $\nu \ll \omega_b \ll \omega$ holds, the expressions for a given bounce mode are as before, but the replacement of the sum on the bounce modes by a bounce integral is unjustified and a profoundly new regime occurs: the decorrelation process now being slow on *all* relevant time scales, global resonances appear, and energy transfer between the wave and the particles is only possible if the wave enters into resonance with global bounce/gyro motion on the poloidally closed orbit. This being unlikely owing to the smallness of ν/ω_b (see also Van Eester 1995), the wave absorption is strongly reduced. In the limit $\nu/\omega_b \to 0^+$, the absorption drops to zero and the so-called superadiabatic regime is reached. This vanishing absorption is at odds with the usual plasma modelling, where the absorption stays finite for vanishing ν. At the outset of the computations in the present paper, only the smallness of ν/ω is implicitly assumed, and both regimes $\nu \ll \omega_b \ll \omega$ and $\omega_b \ll \nu \ll \omega$ are described. When discussing the relation between the model adopted here and the usual plasma models, the less general and thus more questionable condition $\omega_b \ll \nu \ll \omega$ will be used.

Rigorously accounting for the tokamak geometry is not straightforward, and quickly leads to lengthy expressions that are not very transparent. A proper order scheme and a good choice of the independent variables makes the algebra less involved. Using pseudocanonical variables, Balescu (1988) presented an appealing drift ordering method to isolate the fast cyclotron from the much slower guiding-centre motion in the history of a charged particle in a static magnetic field. We base ourselves on his description of the non-perturbed particle evolution, but, unlike Balescu, we limit ourselves to *leading*-order terms in the drift parameter. Kaufman (1972) showed that adopting a set $(\boldsymbol{\Lambda}, \boldsymbol{\Theta})$ of independent variables, where $\boldsymbol{\Lambda}$ are three independent constants of the unperturbed motion and $\boldsymbol{\Phi}$ are three angles that in the absence of RF fields vary linearly with time and describe the oscillatory aspects of the particle motion, allows one to evaluate the dielectric tensor in an elegant way. We take $\boldsymbol{\Lambda} = (\varepsilon, \mu, r_{gc})$, where $\varepsilon = \frac{1}{2}mv^2$ is the energy, $\mu = mv_\perp^2/2B_0(\mathbf{r}_{gc})$ is the magnetic moment evaluated at the guiding centre's position, and r_{gc} is the guiding centre's radial position. The latter is only an approximate constant of the motion. When finite-banana-width effects are retained, the true constant of the motion is the toroidal angular momentum $P = \Psi - 2\pi mRv\,/q$, where Ψ is

https://doi.org/10.1017/S0022377898007016 Published online by Cambridge University Press

the poloidal flux and v the toroidal component of the velocity. In our work, we take the limit of zero banana width. The angles $\mathbf{\Phi} = (\Phi_b, \Phi_d, \Phi_g)$ respectively describe the poloidal bounce motion and the toroidal drift of the guiding centre and the particle's cyclotron gyromotion. Their characteristic frequencies are $\boldsymbol{\omega} = \boldsymbol{\omega}(\mathbf{\Lambda}) = (\omega_b, \omega_d, \omega_g)$. The Jacobian of the transformation from $(\mathbf{r}, \mathbf{v})$ to $(\mathbf{\Lambda}, \mathbf{\Phi})$ is given by

$$J = \frac{\partial \Psi_{gc}/\partial r_{gc}}{2\pi\omega_b m^2}, \tag{1}$$

to leading order in the drift parameter (Van Eester 1995). This transformation is most easily realized using sets of intermediate variables: $(\mathbf{r}, \mathbf{v}) \rightarrow (\mathbf{r}_{gc}, \mathbf{v}) \rightarrow (\mathbf{r}_{gc}, \varepsilon, \mu, \phi) \rightarrow (r_{gc}, \theta_{gc}, \ _{gc}, \varepsilon, \mu, \phi) \rightarrow (\mathbf{\Lambda}, \mathbf{\Phi})$. The explicit expression for the new poloidal coordinate Φ_b for the special case of a tokamak with circular cross-section is given in Appendix A.

Assuming the RF electromagnetic field to be sufficiently small that it causes only small perturbations of the plasma variables, the method of characteristics can be used to find an expression for the RF perturbed distribution function f_{RF}. The perturbed distribution and thus the RF perturbed current density $\mathbf{J}$ are then written as a time-history integral along the unperturbed particle trajectory, and $\mathbf{J}$ is a non-local function of the electric field $\mathbf{E}$ along this orbit. In the weak-decorrelation limit, the time-history integral picks up significant contributions during a very long time period. Owing to the rapid and nearly periodic oscillations and the fact that the weak but finite decorrelation eliminates all contributions very far back in time, only the endpoint contribution appears explicitly in the time-history integral if the decorrelation time is large compared with the cyclotron time but short compared with the bounce time. In that case, the non-local aspects of the wave–particle interaction are unimportant: $f_{RF}(\mathbf{x}, t)$ only depends on $\mathbf{E}$ at the same position and time. This does not imply that the dielectric response is free from poloidal coupling: the partial current density $\mathbf{J}_m$ associated with a given poloidal mode number m involves electric field components from the whole poloidal spectrum and not just $\mathbf{E}_m$. One may then hope that equations exist that, on the one hand, account for the actual particle topology but, on the other, show some resemblance to known results obtained using less sophisticated models. In general models such as those of Kaufman, this resemblance is not always straightforward. The relation between the nonlocal resonance condition associated with a given bounce-spectrum mode in Kaufman's approach and the local resonance condition of straight-magnetic-field-line models is, for example, unclear.

The purpose of this paper is twofold. First, it provides a formalism enabling the study of RF heating in a three-dimensional toroidal but axisymmetrical plasma in the weak-decorrelation limit. The guiding centre rather than the particle position is chosen as the independent variable. Although information on 'local' quantities is lost, the advantage of this approach is that the RF power density in the power balance is directly related to the RF diffusion operator to be used in the associated Fokker–Planck equation. A second and more important goal of this paper is to try to link various formulae and formalisms presented in the literature while discussing the validity of the underlying assumptions.

This paper is structured as follows. First, some general comments on the

https://doi.org/10.1017/S0022377898007016 Published online by Cambridge University Press

Galerkin form of the wave equation are given and the dielectric response in toroidal geometry is discussed (Sec. 2). After that, stationary-phase or fast Fourier transform methods are adopted to evaluate the bounce spectrum (Sec. 3). Section 4 provides some details of and comments on the computation of the dielectric response in the case where the phase of the RF-induced time derivative of the energy is rapidly varying. For practical applications, the most delicate part in the computation of the dielectric response is the evaluation of the bounce spectrum of the interaction of a given orbit with the electric field. A separate subsection (4.1) is devoted to this point. The global link between the bounce spectrum and the bounce integral is discussed in Sec. 4.1; the local violation of the underlying criterion is studied in Sec. 4.2. Explicit formula and a discussion on how the results obtained here are related to existing expressions are provided in Sec. 4.3. In particular, the link is established between the general – but less straightforwardly interpretable – results in the form of a sum on the bounce spectrum due to Kaufman and more familiar – and more directly interpretable – local or bounce-averaged expressions due to various other authors. Finally, conclusions are drawn in Sec. 5.

The accent in this paper is on a critical study of the practical evaluation of the RF diffusion operator and the associated absorbed power density. More details on the associated wave equation and the evaluation of the dielectric response are given in Lamalle (1993, 1994, 1997).

2. The dielectric response W and the associated RF diffusion operator D

The wave equation for a small rapidly varying electric field driven at a frequency in the radiofrequency (RF) range of frequencies and pertinent to toroidal geometry is derived. The usual multiple-time-scale ordering is adopted (see e.g. Bernstein and Baxter 1981). Consequently, the first part of the computation does not differ from other models, so that only a number of points related to the specific choice of independent variables need be discussed in some detail. In contrast to other work, the weak Galerkin form of the wave equation is given in terms of the guiding-centre position rather than the particle position. The advantage of this approach is that the variational form representing the plasma response has a direct physical meaning (absorbed power) and is closely related to the RF diffusion tensor to be used in the Fokker–Planck equation. A disadvantage is that local quantities and operators (such as the RF-induced plasma current or the associated dielectric tensor) are not evaluated.

In its most general form, the wave equation for the rapidly varying RF electric field $\mathbf{E}$ can be written as

$$\boldsymbol{\nabla}\times\boldsymbol{\nabla}\times\mathbf{E} = i\omega\mu_0\mathbf{J}_{\text{total}} + k_0^2\mathbf{E}, \tag{2}$$

in which the current density $\mathbf{J}_{\text{total}}$ is the sum of the externally imposed antenna current density $\mathbf{J}_{\text{ext}}$ on the antenna blades and the RF plasma current

$$\mathbf{J} = \sum_\alpha q_\alpha \int d\mathbf{v}\,\mathbf{v} f_{RF\alpha}.$$

When (i) the RF perturbation is sufficiently small to justify its treatment as a linear perturbation and (ii) finite-banana-width effects are neglected, the

https://doi.org/10.1017/S0022377898007016 Published online by Cambridge University Press

rapidly varying perturbed distribution function, for each of the species α of which the plasma consists, satisfies

$$f_{RF} = -\frac{q}{m}\int_{-\infty}^{t} dt'\,(\mathbf{E}+\mathbf{v}\times\mathbf{B})\cdot\left(\frac{\partial F_0}{\partial\varepsilon}\nabla_{\mathbf{v}}\varepsilon+\frac{\partial F_0}{\partial\mu}\nabla_{\mathbf{v}}\mu+\frac{\partial F_0}{\partial r_{gc}}\nabla_{\mathbf{v}}r_{gc}\right)$$

$$\approx -\frac{q}{m}\left[\frac{\partial F_0}{\partial\varepsilon}\int_{-\infty}^{t} dt'\,m\mathbf{E}\cdot\mathbf{v}+\frac{\partial F_0}{\partial\mu}\int_{-\infty}^{t}\frac{m(\mathbf{E}+\mathbf{v}\times\mathbf{B})\cdot\mathbf{v}_\perp}{B_0}\right.$$

$$\left.+\frac{\partial F_0}{\partial r_{gc}}\int_{-\infty}^{t} dt'\,\frac{1}{\Omega}(\mathbf{E}+\mathbf{v}\times\mathbf{B})\cdot\mathbf{e}_{\perp 2}\right], \tag{3}$$

in which

$$\mathbf{e}_{\perp 2} = \mathbf{e}_\parallel\times\mathbf{e}_r = \frac{\mathbf{B}_0}{B_0}\times\mathbf{e}_{\perp 1},$$

$\mathbf{B}_0$ is the static magnetic field and $\mathbf{e}_{\perp 1} = \mathbf{e}_r$. The integration path is the particle trajectory in absence of the RF fields, and the species subscript α has been dropped. We assume the magnetic surfaces to be circular so that existing analytical expressions for the bounce time can be used. Generalization to a D-shaped geometry can be achieved directly by evaluating the bounce integrals numerically. At the expense of a further complication of the algebra, analytical results may be obtained for non-circular cross-sections. The slowly varying distribution function F_0 is changing on the diffusion time scale, but can be considered constant on both the RF and bounce time scales. It is evaluated by solving the relevant Fokker–Planck equation (for an evaluation of the diffusion operator, see e.g. Van Eester 1995). For an arbitrary distribution function, the first and second terms in (3) are of the same order of magnitude. Using Maxwell's equation $\nabla\times\mathbf{E} = i\omega\mathbf{B}$, it can be seen that the term involving $\partial F_0/\partial r_{gc}$ is small compared with that involving $\partial F_0/\partial\varepsilon$, and can be dropped as a first approximation: for a typical wavenumber k of the perturbed field and scale length L of the equilibrium quantities,

$$m\mathbf{E}\cdot\mathbf{v}\frac{\partial F_0}{\partial\varepsilon} \quad \text{is of order} \quad \frac{F_0 E}{v},$$

$$\frac{\partial F_0}{\partial r_{gc}}\frac{\mathbf{E}\cdot\mathbf{e}_{\perp 2}}{\Omega} \quad \text{is of order} \quad \frac{F_0 E}{L\Omega},$$

$$\frac{\partial F_0}{\partial r_{gc}}\frac{(\mathbf{v}\times\mathbf{B})\cdot\mathbf{e}_{\perp 2}}{\Omega} \quad \text{is of order} \quad \frac{F_0 vkE}{L\Omega\omega},$$

the fourth term in the last line of (3) is of order ρ/L with respect to the first one, while the last is even smaller with respect to the first, since it is of order $\rho^2 k/L \ll 1$. At the cost of a substantial amount of algebra, the radial dependence of F_0 can be accounted for (see e.g. Chen and Tsai 1983; Tsai *et al.* 1984). We underline, however, that the terms involving $\partial/\partial r_{gc}$ do not faithfully describe the RF-induced radial transport, because of the choice of the *approximate* constant of the motion r_{gc} as one of the independent variables: $\nabla_{\mathbf{v}} r_{gc}$ differs from $\nabla_{\mathbf{v}} P$ in both amplitude and direction. The following *approximate*

https://doi.org/10.1017/S0022377898007016 Published online by Cambridge University Press

expression for the perturbed distribution function is therefore appropriate, and will be used in the remainder of the text:

$$f_{RF} = -\frac{\partial F_0}{\partial \varepsilon}\int_{-\infty}^{t} dt'\,\dot{\varepsilon} - \frac{\partial F_0}{\partial \mu}\int_{-\infty}^{t} dt'\,\dot{\mu}; \tag{4}$$

$\dot{\varepsilon}$ and $\dot{\mu}$ are the RF-induced time derivatives of ε and μ:

$$\dot{\varepsilon} = q\mathbf{E}\cdot\mathbf{v}, \qquad \dot{\mu} = \frac{q(\mathbf{E}+\mathbf{v}\times\mathbf{B})\cdot\mathbf{v}_\perp}{B_0}. \tag{5}$$

Using the identity (Landau and Lifshitz 1960)

$$(\mathbf{E}+\mathbf{v}\times\mathbf{B})\,e^{-i\omega t} = \frac{i}{\omega}\left(\frac{d}{dt}\boldsymbol{\nabla}_{\mathbf{v}} - \boldsymbol{\nabla}\right)(\mathbf{E}\cdot\mathbf{v}\,e^{-i\omega t}),$$

one can isolate a term that does not contribute to resonant absorption in the RF-induced time derivative (Lamalle 1994, 1997). Adopting the set of coordinates $(\mathbf{r}_{gc}, \varepsilon, \mu, \phi)$, the perturbed distribution function can then be written as

$$\begin{aligned} f_{RF} &= -\frac{iq\mathbf{E}\cdot\mathbf{v}_\perp}{\omega B_0}\frac{\partial F_0}{\partial \mu} - \int_{-\infty}^{t} dt'\left(\frac{\partial F_0}{\partial \varepsilon} + \frac{iq}{m\omega}\frac{\partial F_0}{\partial \mu}\frac{\partial}{\partial \phi}\right)\dot{\varepsilon} \\ &= -\frac{iq\mathbf{E}\cdot\mathbf{v}_\perp}{\omega B_0}\frac{\partial F_0}{\partial \mu} - \sum_N\left(+\frac{\partial F_0}{\partial \varepsilon} + H_N\frac{\partial F_0}{\partial \mu}\right)\int_{-\infty}^{t} dt'\,\dot{\varepsilon}_N. \end{aligned} \tag{6}$$

The second line is obtained after separating $\dot{\varepsilon}$ into a sum of cyclotron harmonic contributions proportional to $\exp(-iN\phi)$; N is the gyromode number and $H_N = qN/m\omega$. Although the changes to f_{RF} due to RF-induced changes in μ are obscured in (6), this expression is particularly useful for practical applications, since it reduces the number of bounce spectra to be computed to one (that of the RF-induced energy change). Lamalle (1993, 1997) adopted this splitting to write down an elegant general expression for the dielectric response in toroidal geometry and to demonstrate the purely resonant character of the associated absorption.

Since the current density is specified at the particle position $\mathbf{r}$, the above f_{RF} is a function of the particle position $\mathbf{r}$ at which the current is evaluated, and a specific particle velocity $\mathbf{v}$. Aside from this explicit dependence, f_{RF} implicitly involves knowledge of the electric field, $\mathbf{v}'$ and B_0 at positions $\mathbf{r}'$ backwards in time along the zeroth-order trajectory, i.e. the electric field $\mathbf{E}$ and f_{RF} or the current $\mathbf{J}$ are linked via a nonlocal (integral) operator. In the case where f_{RF} only involves the endpoint contribution at $\mathbf{r}$ (see below for a discussion of the conditions defining this regime), the events in the past are irrelevant, and only the end contribution to the time-history integral appears in the final result. The local current density $\mathbf{J}$ then only involves $\mathbf{E}$ at $\mathbf{r}$ (although the local contribution at $\mathbf{r}$ is nonlocal when expressed in terms of $\mathbf{r}_{gc}$, since all orbits intersecting $\mathbf{r}$ contribute). Since the location in six-dimensional space is fully determined, F_0 is to be evaluated for well-defined values of the constants of motion $\boldsymbol{\Lambda}$, namely those characterizing the unique guiding-centre orbit for which the particle location in six-dimensional space is given by $(\mathbf{r}, \mathbf{v})$ at time t:

$$\mathbf{J} = q\int d\mathbf{v}\,\mathbf{v} f_{RF} = q\int d\tilde{\mathbf{r}}\int d\mathbf{v}\,\mathbf{v} f_{RF}\,\delta(\mathbf{r}-\tilde{\mathbf{r}}(\mathbf{r},\mathbf{v})) = q\int d\boldsymbol{\Lambda}\int d\boldsymbol{\Phi}\,J\mathbf{v} f_{RF}\,\delta(\boldsymbol{\Lambda}-\tilde{\boldsymbol{\Lambda}}(\mathbf{r},\mathbf{v})).$$

https://doi.org/10.1017/S0022377898007016 Published online by Cambridge University Press

Although this remark may seem trivial at first sight, it has important implications: when computing the dielectric response, one must start from F_0 specified at the guiding-centre position corresponding to the *imposed* $(\mathbf{r}, \mathbf{v})$, and thus the angle integrals performed afterwards then sum on all possible

(i) guiding centres contributing to the current at $\mathbf{r}$ when adopting $(\mathbf{r}, \mathbf{v})$ as independent variables; or
(ii) particles sharing the same guiding centre but contributing to the current at various $\mathbf{r}$ when adopting $(\mathbf{r}_{gc}, \mathbf{v})$ as independent variables.

In the first case, the obtained dielectric response is local in particle space but non-local in guiding-centre space, and one has to rewrite $F_0(\mathbf{\Lambda})$ in terms of local quantities using a Taylor series expansion before performing the velocity integral (see e.g. Martin *et al.* 1987; Romero *et al.* 1987). In the case where the second option is preferred, the tedious Taylor expansion is unnecessary, but, since the dielectric response is expressed in terms of $\mathbf{r}_{gc}$, local information at $\mathbf{r}$ is sacrificed and, for example, the current or the dielectric tensor are never actually computed. That the two approaches are two equivalent representations of the wave problem is seen when formulating the problem variationally. Multiplying the current by the complex conjugate of a sufficiently smooth test-function vector $\mathbf{F}$ and integrating over the total volume, one gets

$$\int d\mathbf{r}\, \mathbf{F}^* \cdot \mathbf{J} = q \int d\mathbf{r}\, \mathbf{F}^* \cdot \int d\mathbf{v}\, \mathbf{v} f_{RF} \approx q \int d\mathbf{\Lambda} \int d\mathbf{\Phi}\, J \mathbf{F}^* \cdot \mathbf{v} f_{RF}$$

('$\approx$' because J is the Jacobian to leading order in the drift parameter in this paper). Multiplying the whole wave equation by the complex conjugate of the test-function vector $\mathbf{F}$ and integrating it over the total volume of the tokamak, consisting of a metallic shell containing a central plasma region surrounded by a vacuum zone in which an RF antenna is situated, results in the weak Galerkin form of the wave equation

$$\int d\mathbf{r}[(\nabla \times \mathbf{F})^* \cdot (\nabla \times \mathbf{E}) - k_0^2 \mathbf{F}^* \cdot \mathbf{E}] = i\omega\mu_0 \int d\mathbf{x}\, \mathbf{F}^* \cdot \mathbf{J}_{\text{ext}} + \mathsf{W} + \text{surface term}, \quad (7)$$

where the surface term is obtained via a partial integration and represents the Poynting flux when $\mathbf{E}$ is substituted for $\mathbf{F}$. The second term on the right-hand side describes the just-discussed dielectric response of the plasma to an RF perturbation driven by $\mathbf{J}_{\text{ext}}$. The dielectric response is expressed most elegantly in terms of the guiding-centre variables. A suitable expression for it is

$$\mathsf{W} = \int\int d\mathbf{x}_6\, \mathsf{W}_6(\mathbf{F}, \mathbf{E}) \quad (8a)$$

in which $\mathbf{x}_6 = (\mathbf{\Lambda}, \mathbf{\Phi})$ and

$$\mathsf{W}_6(\mathbf{F}, \mathbf{E}) = -i\omega\mu_0 J q \mathbf{F}^* \cdot \mathbf{v} \left(\frac{\partial F_0}{\partial \varepsilon} \int_{-\infty}^{t} dt'\, \dot{\varepsilon} + \frac{\partial F_0}{\partial \mu} \int_{-\infty}^{t} dt'\, \dot{\mu} \right). \quad (8b)$$

The total absorbed power is

$$\frac{1}{2} \text{Re} \left[\int\int d\mathbf{x}_6 \frac{\mathsf{W}_6(\mathbf{E}, \mathbf{E})}{i\omega\mu_0} \right],$$

https://doi.org/10.1017/S0022377898007016 Published online by Cambridge University Press

and $\mathsf{W}_6(\mathbf{E},\mathbf{E})/2i\omega\mu_0$ is the complex absorbed power density associated with the guiding-centre orbit $\mathbf{\Lambda}$. In the above, both the electric field $\mathbf{E}$ and the test function $\mathbf{F}$ are evaluated at the particle position at the outset. The RF-induced time derivatives of the energy, the magnetic moment and $\mathbf{F}^*\cdot\mathbf{v}$ can be written in terms of their values at the guiding-centre coordinates using the Taylor expansion $\mathbf{r}=\mathbf{r}_{gc}+\boldsymbol{\rho}$ of the particle's position around its guiding centre:

$$\mathbf{H}(\mathbf{r},t)=\mathsf{L}\mathbf{H}(\mathbf{r}_{gc},\mathbf{v},t),\qquad\text{or}\qquad\mathbf{H}(\mathbf{r}_{gc},\mathbf{v},t)=\mathsf{L}^{-1}\mathbf{H}(\mathbf{r},t). \tag{8c}$$

Note that the identity $\mathbf{H}=\mathsf{L}\mathsf{L}^{-1}\mathbf{H}$ must hold. In our model, only leading-order terms in the drift parameter are retained. Consequently, the *variations* of $\boldsymbol{\rho}$ with respect to $\mathbf{r}_{gc}$ are neglected, and the operators L and L^{-1} are the differential operators

$$\mathsf{L}=\exp(\boldsymbol{\rho}\cdot\boldsymbol{\nabla})=1+\boldsymbol{\rho}\cdot\boldsymbol{\nabla}+\frac{1}{2!}(\boldsymbol{\rho}\cdot\boldsymbol{\nabla})^2+\ldots,$$

$$\mathsf{L}^{-1}=\exp(-\boldsymbol{\rho}\cdot\boldsymbol{\nabla})=1-\boldsymbol{\rho}\cdot\boldsymbol{\nabla}+\frac{1}{2!}(\boldsymbol{\rho}\cdot\boldsymbol{\nabla})^2+\ldots,$$

which act on $\mathbf{H}$ only. They can be manipulated using formulae such as $e^{d/d\xi}[AB]=e^{d/d\xi}[A]\,e^{d/d\xi}[B]$. The Galerkin form (7) of the wave equation allows one to find the electric field $\mathbf{E}$. The wave equation itself follows from the requirement that $\mathbf{E}$ should satisfy (7) for a sufficiently smooth but otherwise arbitrary $\mathbf{F}$. It is found most easily by removing the differential operators in L acting on $\mathbf{F}$ in (8*b*–*c*). This involves performing partial integrations, and gives rise to extra surface terms:

$$\mathsf{W}=\int d\mathbf{x}_6\,\mathbf{F}^*\cdot\mathbf{W}\cdot\mathbf{E}+\text{surface terms}, \tag{8d}$$

in which $\mathbf{W}$ is a differential operator and both $\mathbf{E}$ and $\mathbf{F}$ are evaluated at the guiding centre rather than the particle position. Since $\mathbf{F}$ is an arbitrary test function, the wave equation is just given by setting equal to zero the expression multiplying $\mathbf{F}^*$ (i.e. $\mathbf{W}\cdot\mathbf{E}$ + a term coming from the $\boldsymbol{\nabla}\times\boldsymbol{\nabla}\times$ operator) in the volume terms of the Galerkin form. When $\mathbf{E}$ is substituted for $\mathbf{F}$, the surface term in the above is a 'kinetic' flux (in the sense that it is proportional to the density) at the guiding-centre position. Note that, unlike what is usually done, neither the dielectric tensor nor the kinetic flux at the particle position are ever evaluated. When integrating over the total volume and using sufficiently smooth test functions $\mathbf{F}$, the surface terms do not explicitly appear in the Galerkin form, since the total (kinetic + Poynting) flux is continuous in the plasma and in the vacuum layer. It vanishes at the metallic boundary surrounding the plasma: the kinetic flux is zero since the tangential electric field vanishes, while the Poynting flux is zero because of the absence of particles in that region. Only at the plasma–vacuum interface do the surface terms have to be included explicitly, because of the continuity of the total flux. The kinetic flux is the difference between the work done by the field on the particles in a fixed volume and the actual complex power $\mathsf{W}/2i\omega\mu_0$ transferred from the fields to the particles, excluding the artificial 'heating' due to the in- or outflow of particles into or out of the fixed reference volume: As discussed for example in Václavík and Appert (1987), evaluating the change of energy ('heating') of a

https://doi.org/10.1017/S0022377898007016 Published online by Cambridge University Press

group of particles requires *modifying* the reference volume so as to fix the set of reference particles, rather than fixing the reference volume. The plasma heating is indeed given by

$$\left.\frac{\partial}{\partial t}\right|_{RF}\int d\mathbf{\Lambda}\int d\mathbf{\Phi}\, J\varepsilon F_0(r_{gc},\varepsilon,\mu) = (2\pi)^3\int d\mathbf{\Lambda}\, J\varepsilon \left.\frac{\partial F_0}{\partial t}\right|_{RF},$$

where

$$\left.\frac{\partial F_0}{\partial t}\right|_{RF} =$$

$$\mathsf{D}F_0 = \frac{1}{2J}\mathrm{Re}\left\{\begin{pmatrix}\frac{\partial}{\partial\varepsilon} & \frac{\partial}{\partial\mu}\end{pmatrix} J \begin{pmatrix} \dot\varepsilon^* \int_{-\infty}^{t} dt'\,\dot\varepsilon & \dot\varepsilon^* \int_{-\infty}^{t} dt'\,\dot\mu \\ \dot\mu^* \int_{-\infty}^{t} dt'\,\dot\varepsilon & \dot\mu^* \int_{-\infty}^{t} dt'\,\dot\mu \end{pmatrix} \begin{pmatrix}\frac{\partial}{\partial\varepsilon} \\ \frac{\partial}{\partial\mu}\end{pmatrix}\right\} F_0, \quad (8e)$$

with D the RF diffusion operator, and thus, after a partial integration,

$$P_{\mathrm{abs}} = \int\int d\mathbf{x}_6\, J\varepsilon \mathsf{D}F_0. \quad (8f)$$

The radial derivatives, responsible for RF-induced radial transport, have again been neglected for the same reasons that were used to arrive at (4). Their omission allows one to find an 'isolated' solution of the Fokker–Planck equation on each magnetic surface $r_{gc} = \mathrm{const}$. Using the procedure that was adopted in order to arrive at (6) to isolate terms in $\dot\mu$ that do not contribute to absorption, and taking advantage of the orthogonality of the cyclotron harmonic modes, the RF diffusion operator can be written more compacty as

$$\mathsf{D}F_0 = \frac{1}{J}\begin{pmatrix}\frac{\partial}{\partial\varepsilon} & \frac{\partial}{\partial\mu}\end{pmatrix} J \sum_N \frac{1}{2}\mathrm{Re}\left\{\dot\varepsilon_N^* \int_{-\infty}^{t} dt'\,\dot\varepsilon_N\right\}\begin{pmatrix}1 & H_N \\ H_N & H_N^2\end{pmatrix}\begin{pmatrix}\frac{\partial}{\partial\varepsilon} \\ \frac{\partial}{\partial\mu}\end{pmatrix} F_0, \quad (8g)$$

Equation (7) differs from usual Galerkin forms for solving the wave equation in that the guiding-centre coordinates rather than the particle coordinates are used as the independent variables. With this choice of variables, the elementary dielectric response appears in the Galerkin functional in the form of the absorbed power density per guiding-centre orbit, which is a quantity directly related to the RF diffusion operator used in the associated Fokker–Planck equation. For our specific choice of independent variables, W can be written as

$$\mathsf{W} = -\frac{i\omega\mu_0}{2\pi m^2}\int dr_{gc}\frac{\partial\Psi_{gc}}{\partial r_{gc}}\int d\varepsilon\int d\mu\frac{1}{\omega_b}\int d\mathbf{\Phi}\, q\mathbf{F}^*\cdot\mathbf{v}\left(\frac{\partial F_0}{\partial\varepsilon}\int_{-\infty}^{t} dt'\,\dot\varepsilon + \frac{\partial F_0}{\partial\mu}\int_{-\infty}^{t} dt'\,\dot\mu\right). \quad (9)$$

As Kaufman explained, the evaluation of the integrals over $\mathbf{\Phi} = \Phi_d, \Phi_g, \Phi_b)$ is straightforward when the $\mathbf{\Phi}$ Fourier spectra of $\dot\varepsilon$, $\dot\mu$ and $q\mathbf{F}^*\cdot\mathbf{v}$ are known. The RF modelling can then be subdivided into two separate parts:

(i) *The evaluation of the Fourier spectra of $\dot\varepsilon$ and $\dot\mu$ at a fixed time t.* Some details of this will be given in the next section. Strictly, this first part involves the details of a 1-to-1 coordinate transformation; it does *not* describe any of the actual RF heating physics.

https://doi.org/10.1017/S0022377898007016 Published online by Cambridge University Press

(ii) *The evaluation of the dielectric response and the associated RF diffusion operator*. In this part, the actual physics problem (and effects such as particle decorrelation) is addressed.

When an expression for the Fourier amplitudes at fixed time t is known, we can evaluate the dielectric response (9). It is a double sum over the bounce modes $\mathbf{m}$ of $\mathbf{E}\cdot\mathbf{v}$ and $\mathbf{m}'$ of $\mathbf{F}^*\cdot\mathbf{v}$, but since $\dot{\mathbf{\Phi}} = \boldsymbol{\omega}$ and assuming decorrelation can be accounted for by adding a small but finite positive imaginary part to the driver frequency ω to ensure causality, the time integrals are

$$\exp[i(\mathbf{m}\cdot\mathbf{\Phi}-\omega t)]\int_{-\infty}^{0} d\tau \exp[i(\mathbf{m}\cdot\boldsymbol{\omega}-\omega)\tau] = \frac{\exp[i(\mathbf{m}\cdot\mathbf{\Phi}-\omega t)]}{i(\mathbf{m}\cdot\boldsymbol{\omega}-\omega)}.$$

This simple decorrelation model amounts to adding an attenuation factor $e^{\nu t}$ to the Vlasov equation. This attenuation factor models the reduced importance of the events in the far past. More sophisticated decorrelation models replace the attenuation factor and consequently the resonant denominator by another function (see e.g. Kasilov *et al.* 1990; Catto *et al.* 1993; Brambilla 1994), but a fully rigorous treatment of the coupling of the fast and slow time scales is still awaited. Such a treatment of the decorrelation is only possible when solving the Vlasov and Fokker–Planck equations together, which requires accounting for variations in the Vlasov equation that do not play a significant role on the fast time scale, but whose cumulative effects cannot be neglected when performing the time-history integral up to a point very far back in the past (for a qualitative discussion, see e.g. Van Eester *et al.* 1996). Since such detailed descriptions are presently unavailable, the mixing of the effects on the different time scales in the problem is mocked up by – more or less physically justified – attenuation factors.

The integral over the angles $\mathbf{\Phi}$ eliminates all contributions for which $\mathbf{m} \neq \mathbf{m}'$, and thus the dielectric response can be written in the form

$$\mathsf{W} = -\omega\mu_0\left(\frac{2\pi}{m}\right)^2 \int dr_{gc}\frac{\partial\Psi_{gc}}{\partial r_{gc}}\int d\varepsilon\int d\mu\frac{1}{\omega_b}\sum_{\mathbf{m}}\frac{q\mathbf{F}^*\cdot\mathbf{v}_{\mathbf{m}}\left(\dfrac{\partial F_0}{\partial\varepsilon}\dot{\varepsilon}_{\mathbf{m}}+\dfrac{\partial F_0}{\partial\mu}\dot{\mu}_{\mathbf{m}}\right)}{\mathbf{m}\cdot\boldsymbol{\omega}-\omega}. \quad (10)$$

We note that $\mathbf{m}$ is the vector of bounce mode numbers. Aside from the simple sum on $\mathbf{m}$ that appears explicitly in (10), a sum on the usual poloidal modes is hidden in each of the Fourier amplitudes $\mathbf{E}\cdot\mathbf{v}$ and $\mathbf{F}^*\cdot\mathbf{v}$ (see Sec. 3). From $(8e,g)$, the quasilinear diffusion term consistent with (10) to be used in the Fokker–Planck equation is found to be

$$\mathsf{D}F_0 = \frac{1}{2J}\mathrm{Re}\left\{\begin{pmatrix}\dfrac{\partial}{\partial\varepsilon} & \dfrac{\partial}{\partial\mu}\end{pmatrix}J\sum_{\mathbf{m}}\frac{1}{i(\mathbf{m}\cdot\boldsymbol{\omega}-\omega)}\begin{pmatrix}\dot{\varepsilon}^*_{\mathbf{m}}\dot{\varepsilon}_{\mathbf{m}} & \dot{\varepsilon}^*_{\mathbf{m}}\dot{\mu}_{\mathbf{m}}\\ \dot{\mu}^*_{\mathbf{m}}\dot{\varepsilon}_{\mathbf{m}} & \dot{\mu}^*_{\mathbf{m}}\dot{\mu}_{\mathbf{m}}\end{pmatrix}\begin{pmatrix}\dfrac{\partial}{\partial\varepsilon}\\ \dfrac{\partial}{\partial\mu}\end{pmatrix}\right\}F_0$$

$$= \frac{1}{J}\begin{pmatrix}\dfrac{\partial}{\partial\varepsilon} & \dfrac{\partial}{\partial\mu}\end{pmatrix}J\sum_{\mathbf{m}}\frac{1}{2}\mathrm{Re}\left\{\frac{1}{i(\mathbf{m}\cdot\boldsymbol{\omega}-\omega)}\right\}|\dot{\varepsilon}_{\mathrm{m}}|^2\begin{pmatrix}1 & H_N\\ H_N & H_N^2\end{pmatrix}\begin{pmatrix}\dfrac{\partial}{\partial\varepsilon}\\ \dfrac{\partial}{\partial\mu}\end{pmatrix}F_0. \quad (11)$$

https://doi.org/10.1017/S0022377898007016 Published online by Cambridge University Press

The latter expression is consistent with the Hamiltonian formalism. Up to a constant factor, $\dot{\varepsilon}_{\mathbf{m}}$ is the perturbed Hamiltonian $\mathsf{H}_{\mathbf{m}}$ for the bounce mode characterized by $\mathbf{m}$ (see e.g. Eriksson and Helander 1994; Carlsson *et al.* 1997):

$$-\frac{\partial}{\partial t}\mathsf{H}_{\mathbf{m}} = \dot{\varepsilon}_{\mathbf{m}}.$$

The approach adopted in this paper has some similarities with the gyrokinetic approach of Chen and Tsai (Chen and Tsai 1983; Tsai *et al.* 1984). Unlike what is done here, however, these authors retain a two-dimensional spatial dependence in F_0 in their model and go beyond tokamak geometry: aside from its dependence on the energy and the magnetic moment, their F_0 depends on the perpendicular guiding-centre position. This leads to a rather involved formalism prohibiting easy comparison of results. In the tokamak case, the amount of algebra is significantly reduced. Adopting the formalism based on the works of Kaufman, not only are more symmetrical and transparent results obtained, but also finite-banana-width effects can be included. Since the latter means that one accounts for the fact that the guiding centres are not tied to a single magnetic surface, which further complicates the tedious evaluation of the Fourier amplitudes of the RF-induced time derivates of $\mathbf{\Lambda}$, this effect was omitted in the present paper, although a *formal* inclusion of the drift effects is rather straightforward: it suffices to add one term to the operator acting on F_0 in (6) and to add a third dimension to the RF diffusion operator (8) (for a clear discussion of this subject, see Eriksson and Helander 1994). Comparing equation (69) in Chen and Tsai (1983) and equation (10) in Lamalle (1993), one notes that the supplementary difficulty the radial extent of the guiding-centre orbits adds to the problem, is evaded by Chen and Tsai by replacing the actual constant of the motion P by the approximate constant Ψ.

3. Evaluation of the Fourier amplitudes associated with the angles $\mathbf{\Phi}$

In this section, it is explained how the complex Fourier amplitudes of the RF-induced time derivative of quantities such as the energy and the magnetic moment can be computed at a fixed time t. Using the local Cartesian frame ($\mathbf{e}_{\perp 1}$, $\mathbf{e}_{\perp 2}, \mathbf{e}_{\parallel}$), introduced earlier $\mathbf{v}$ can be written as

$$\mathbf{v} = \mathbf{v}_{\parallel} + \mathbf{v}_{\perp} = v_{\parallel}\,\mathbf{e}_{\parallel} + v_{\perp}(\cos\phi\,\mathbf{e}_{\perp 1} + \sin\phi\,\mathbf{e}_{\perp 2}),$$

where ϕ is the gyrophase. In the drift approximation ordering, the particle motion is subdivided into two parts: the motion of the guiding centre and the much more rapid cyclotron oscillation of the particle around the guiding centre. Both $v_{\parallel}$ and $v_{\perp}$ undergo variations on the slower time scale resulting from the inhomogeneity of the magnetic field (see e.g. Balescu 1988). Dropping the derivatives of the unit vectors and the slowly varying Larmor radius in comparison with those of the rapidly varying phase ϕ, the particle and guiding-centre positions are related via

$$\mathbf{r} \approx \mathbf{r}_{gc} + \boldsymbol{\rho}(\mathbf{r}_{gc}, \phi) = \mathbf{r}_{gc} + \rho(-\sin\phi\,\mathbf{e}_{\perp 1} + \cos\phi\,\mathbf{e}_{\perp 2}), \tag{12}$$

in which the time derivative of the particle velocity's phase $\phi, \dot{\phi} \approx -\Omega$, is evaluated at the guiding centre rather than the particle position, and

https://doi.org/10.1017/S0022377898007016 Published online by Cambridge University Press

$\rho = v_\perp/\Omega$ is the Larmor radius. Abbreviating the $\mathbf{m}$ Fourier components of $\mathbf{H}\cdot\mathbf{v}$ and $\mathbf{H}\cdot\mathbf{v}_\perp/B_0$ ($\mathbf{H} = \mathbf{E}$ or $\mathbf{F}$*) as $\mathscr{H}_\mathbf{m}$ and $\tilde{\mathscr{H}}_\mathbf{m}$,

$$\begin{Bmatrix} \mathscr{H}_\mathbf{m} \\ \tilde{\mathscr{H}}_\mathbf{m} \end{Bmatrix} = \frac{1}{(2\pi)^3}\int_0^{2\pi} d\Phi_b \int_0^{2\pi} d\Phi_d \int_0^{2\pi} d\Phi_g \exp(-i\mathbf{m}\cdot\mathbf{\Phi}) \begin{Bmatrix} \mathbf{H}\cdot\mathbf{v} \\ \dfrac{\mathbf{H}\cdot\mathbf{v}_\perp}{B_0} \end{Bmatrix},$$

one readily finds

$$\begin{Bmatrix} \mathscr{H}_\mathrm{m} \\ \tilde{\mathscr{H}}_\mathbf{m} \end{Bmatrix} = \sum_m \sum_n \frac{\delta(n-m_d)}{2\pi}\int_0^{2\pi} d\Phi_b \exp\left\{ i\left[(m\delta_{tp} - m_b)\Phi_b + \sum_{l=1}^{\infty} \xi_{l,m_g} \sin(l\Phi_b) - \omega t \right]\right\}$$
$$\times \left[\begin{Bmatrix} 1 \\ \dfrac{1}{B_0} \end{Bmatrix} \frac{v_\perp}{2} \{ \exp[i(1-m_g)\psi] J_{1-m_g}(\chi) H_- \right.$$
$$+ \exp[-i(1+m_g)\psi] J_{-1-m_g}(\chi) H_+ \}$$
$$\left. + \begin{Bmatrix} v_\parallel \exp(-im_g\psi) J_{-m_g}(\chi) H_\parallel \\ 0 \end{Bmatrix} \right]. \tag{13}$$

The orthogonality of the Φ_d Fourier modes imposes $n = m_d$, while the orthogonality of the Φ_g Fourier modes requires that the cyclotron harmonic number N be $-m_g$. Details can be found in Appendix B.

The evaluation of the above bounce integrals is a tedious exercise, since, aside from the explicit dependence of the exponential factor on the bounce angle Φ_b, the factors $v_\perp$, $v_\parallel$, ψ and χ are not constant poloidally. The differential operators in the above are all of the form $\exp(iL\Psi) J_L$, which can formally be expanded in Taylor series (Abramowitz and Stegun 1972). Explicitly, they can be written as

$$\exp(iL\psi) J_L = \left(\frac{-i\rho}{2}\right)^L \nabla_-^L \sum_{j=0} \left(\frac{\rho}{2}\right)^{2j} \frac{\Delta_\perp^j}{j!(L+j)!}, \tag{14a}$$

$$\exp(-iL\psi) J_{-L} = \left(\frac{i\rho}{2}\right)^L \nabla_+^L \sum_{j=0} \left(\frac{\rho}{2}\right)^{2j} \frac{\Delta_\perp^j}{j!(L+j)!}, \tag{14b}$$

in which L is positive or zero and the notation

$$\nabla_\pm = \frac{d}{dr_{gc}} \pm k_{\perp 2}, \tag{14c}$$

$$\Delta_\perp = \nabla_+\nabla_- = \frac{d^2}{dr_{gc}^2} - k_{\perp 2}^2 \tag{14d}$$

has been introduced.

The formulae obtained allow one to evaluate the amplitudes of the bounce spectra of the RF-induced time derivatives of the energy and the magnetic moment. Before being able to make practical use of them, the bounce integral in (13) must be performed. Two regimes are distinguished: the Čerenkov regime and the cyclotron regime.

When $m_g = 0$ (Čerenkov interaction) and for not too large m and n, the phase of the exponential in (13) varies slowly. In that case, a few terms in the Fourier expansion of the guiding-centre motion suffice to describe this motion accurately. Two methods have been proposed to evaluate the bounce integrals

https://doi.org/10.1017/S0022377898007016 Published online by Cambridge University Press

for that case. The first relies on using the fast Fourier transform, and is documented in Louis (1996, 1998; Louis and Lamalle 1996). The second uses the periodicity of the time variation of the guiding-centre motion and the gyrophase, and is based on performing the bounce integral analytically by repeatedly making use of (B 1) (see Appendix B). This results in multiple sums of the form $\exp(i\nu\Phi_b)$, the integration of which is immediate (see Van Eester 1995). In practice, the bounce integral can be evaluated analytically provided the number of terms is not too large. Looking at the dominant term in the expansion of the Bessel function for large ν but for a fixed argument ξ (Abramowitz and Stegun 1972),

$$J_\nu(\xi) \approx \frac{1}{(2\pi\nu)^{1/2}}\left(\frac{e\xi}{2\nu}\right)^\nu,$$

it can be seen that the infinite sums can be truncated at $\nu = \nu_{\max}$ somewhat larger than $C\xi$, where C is a constant exceeding $\frac{1}{2}e \approx 1.359$.

When, on the other hand, $m_g \neq 0$ (cyclotron interaction), $\xi_{l,\nu} \gg 1$ (ω_g/ω_b is typically of order 1000) and the exponential in (13) is rapidly oscillating. The stationary-phase method then is perfectly suited for the evaluation of the bounce integrals (see also Lamalle 1994, 1997; Louise 1996; Louis and Lamalle 1996). All integrals in the bounce amplitudes are now of the general form

$$I = \frac{1}{2\pi}\int_0^{2\pi} d\Phi_b\, \mathcal{G}(\Phi_b)\exp(i\Theta), \tag{15}$$

in which $\mathcal{G}$ is a slowly varying function of the bounce angle Φ_b, and the phase Θ is given by

$$\begin{aligned}\Theta &= m\theta_{gc} + n\ \ _{gc} + m_g\phi - \mathbf{m}\cdot\mathbf{\Phi} = m\theta_{gc} + n\left(\ \ _{gc} - \langle\ \dot{}\ _{gc}\rangle\frac{\Phi_b}{\omega_b}\right)\\ &\quad + m_g\left(\phi - \langle\dot{\phi}\rangle\frac{\Phi_b}{\omega_b}\right) - m_b\,\Phi_b\\ &= (m\delta_{tp} - m_b)\,\Phi_b + \sum_{l=1}^{\infty}\xi_{l,m_g}\sin(l\Phi_b).\end{aligned} \tag{16}$$

Since the factor ξ_{l,m_g} is large, Θ is rapidly varying. Evaluating the integral using the method of stationary phase, one readily gets

$$I \approx \sum_{SPP}\mathcal{G}\frac{\exp\{i[\Theta + \frac{1}{4}\pi - \frac{1}{2}\arg(\Theta'')]\}}{(2\pi)^{1/2}|\Theta''|^{1/2}}, \tag{17}$$

where $' = \partial/\partial\Phi_b$ and all quantities are evaluated at the stationary phase points, whose position is given by

$$\Theta' = m\delta_{tp} - m_b + \sum_{l=1}^{\infty} l\xi_{l,m_g}\cos(l\Phi_b) = 0, \tag{18}$$

which relates m_b to the stationary-phase angle:

$$m_b = \frac{m\dot{\theta}_{gc} + n(\ \dot{}\ _{gc} - \langle\ \dot{}\ _{gc}\rangle) + m_g(\dot{\phi} - \langle\dot{\phi}\rangle)}{\omega_b} = m\delta_{tp} + \sum_{l=1}^{\infty} l\xi_{l,m_g}\cos(l\Phi_{b,SPP}). \tag{19}$$

https://doi.org/10.1017/S0022377898007016 Published online by Cambridge University Press

It is important to note that the stationary-phase points do *not* depend on frequency: they appear when computing the Fourier amplitudes for a new set of angles $\mathbf{\Phi}$ at a given time t in order to facilitate the evaluation of the dielectric response. At this stage of the computation, they thus have, in particular, nothing to do with the cyclotron resonance condition. Another important remark is that (17) does not predict the correct value of the integral if the second derivative of the phase vanishes. In such a case, the Taylor series expansion of the phase has to be carried out through one order higher. One gets (Abramowitz and Stegan 1972)

$$I \approx \mathrm{sign}(\ddot{\Theta}_{tp})\,\mathscr{G}\exp(i\Theta_{tp})\frac{\mathrm{Ai}(z)}{|\frac{1}{2}\dddot{\Theta}_{tp}|^{1/3}}, \tag{20}$$

in which the argument z of the Airy function is $-|\dot{\Theta}_{tp}\,2^{1/3}/\ddot{\Theta}_{tp}^{1/3}|$ when expressed in terms of the values of the derivatives at the turning-point position, or $-|\ddot{\Theta}_{sp}^{2}/2^{2/3}\dddot{\Theta}_{sp}^{4/3}|$ when written in terms of the derivatives at either of the nearby stationary-phase points (see e.g. Stix 1975; Bécoulet *et al.* 1991; Lamalle 1994, 1997). As it should, the expression (17) agrees with (20) when $|z|$ is large. In terms of the usual coordinates and time, the stationary-phase condition becomes

$$m\dot{\theta}_{gc} + n\dot{\zeta}_{gc} + m_g\dot{\phi} = \mathbf{m}\cdot\boldsymbol{\omega}. \tag{21}$$

and so the dielectric response (10) can be rewritten in the more familiar form

$$\mathsf{W} = -\omega\mu_0\left(\frac{2\pi}{m}\right)^2\int dr_{gc}\frac{\partial\Psi_{gc}}{\partial r_{gc}}\int d\varepsilon\int d\mu\frac{1}{\omega_b}\sum_{\mathbf{m}}\frac{q\mathbf{F}^*\cdot\mathbf{v}_{\mathbf{m}}\left(\dfrac{\partial F_0}{\partial\varepsilon}\dot{\varepsilon}_{\mathbf{m}}+\dfrac{\partial F_0}{\partial\mu}\dot{\mu}_{\mathbf{m}}\right)}{m\dot{\theta}_{gc}+n\dot{\zeta}_{gc}+m_g\dot{\phi}-\omega}, \tag{22}$$

where the resonant denominator is $k_\parallel v_\parallel - m_g\Omega - \omega$, and the whole expression is to be evaluated at the stationary-phase point. The associated RF diffusion term is

$$\begin{aligned}\left.\frac{\partial F_0}{\partial t}\right|_{RF} = \mathsf{D}F_0 &= \frac{1}{2J}\mathrm{Re}\left\{\left(\frac{\partial}{\partial\varepsilon}\quad\frac{\partial}{\partial\mu}\right)J\right.\\ &\left.\times\sum_{\mathbf{m}}\frac{1}{i(m\dot{\theta}_{gc}+n\dot{\zeta}_{gc}+m_g\dot{\phi}-\omega)}\begin{pmatrix}\dot{\varepsilon}_{\mathbf{m}}^*\dot{\varepsilon}_{\mathbf{m}} & \dot{\varepsilon}_{\mathbf{m}}^*\dot{\mu}_{\mathbf{m}}\\ \dot{\mu}_{\mathbf{m}}^*\dot{\varepsilon}_{\mathbf{m}} & \dot{\mu}_{\mathbf{m}}^*\dot{\mu}_{\mathbf{m}}\end{pmatrix}\begin{pmatrix}\dfrac{\partial}{\partial\varepsilon}\\ \dfrac{\partial}{\partial\mu}\end{pmatrix}\right\}F_0\\ &= \frac{1}{2J}\mathrm{Re}\left(\frac{\partial}{\partial\varepsilon}\frac{\partial}{\partial\mu}\right)J\sum_{\mathbf{m}}\frac{|\dot{\varepsilon}_{\mathbf{m}}|^2}{i(m\dot{\theta}_{gc}+n\dot{\zeta}_{gc}+m_g\dot{\phi}-\omega)}\begin{pmatrix}1 & -H_{m_g}\\ -H_{m_g} & H_{m_g}^2\end{pmatrix}\begin{pmatrix}\dfrac{\partial}{\partial\varepsilon}\\ \dfrac{\partial}{\partial\mu}\end{pmatrix}F_0,\end{aligned} \tag{23}$$

where terms not giving rise to resonant absorption have been isolated to find the latter expression.

Eliminating m_b, the phase at the stationary-phase point is

$$\Theta(\Phi_{b,SPP}) = m\left(\theta_{gc}-\langle\dot{\theta}_{gc}\rangle\frac{\Phi_b}{\omega_b}\right)+n\left(\zeta_{gc}-\langle\dot{\zeta}_{gc}\rangle\frac{\Phi_b}{\omega_b}\right)+m_g\left(\phi-\langle\dot{\phi}\rangle\frac{\Phi_b}{\omega_b}\right).$$

https://doi.org/10.1017/S0022377898007016 Published online by Cambridge University Press

This phase only contains contributions from the *periodic* (nonlinear) part of the guiding-centre and gyromotion. It goes to zero when the magnetic-mirror acceleration due to the inhomogeneity of the static magnetic field is absent, in which case the particle motion is *formally* as in a uniform plasma: constant poloidal and toroidal velocities and gyrofrequency so that guiding-centre and gyro angles grow *linearly* with time. The expression for $\mathscr{H}_{\mathbf{m}}$ is

$$\mathscr{H}_{\mathbf{m}} = \frac{1}{(2\pi)^{1/2}} \sum_m \sum_n \delta(n - m_d) \sum_{SPP} \exp[i(\tfrac{1}{4}\pi - \omega t)] \frac{\exp\{i[\Theta - \frac{1}{2}\arg(\Theta'')]\}}{|\Theta''|^{1/2}}$$
$$\times \{\tfrac{1}{2} v_\perp \{\exp[i(1-m_g)\psi] J_{1-m_g}(\chi) H_- + \exp[-i(1+m_g)\psi] J_{-1-m_g}(\chi) H_+\}$$
$$+ v_\parallel \exp(-i m_g \psi) J_{-m_g}(\chi) H_\parallel\},$$

in which all quantities $(v_\perp, v_\parallel, \ldots)$ are evaluated at the stationary-phase position. For fixed $\mathbf{m}$, only one gyromode $N = -m_g$ and one toroidal mode $n = m_d$ appears, because the equilibrium is uniform toroidally, but many poloidal bounce modes contribute as a consequence of the poloidal inhomogeneity felt by the particle on its helicoidal orbit. Only those m_g for which the stationary-phase condition is satisfied somewhere in the plasma need be retained.

When $m_g \neq 0$, the bounce integral can equally be evaluated by repeatedly using (B 1) from Appendix B, but the number of terms to be evaluated quickly becomes so large that its use cannot be recommended for numerical applications. Although seemingly based on rather different assumptions, both methods are equivalent for sufficiently rapid phase variations (Van Eester 1995).

The case $r_{gc} \approx 0$ is a special case for which the complication of the poloidal inhomogeneity nearly disappears. The relevant expressions are closely related to those obtained for the straight-magnetic-field-line geometry, but include toroidicity effects (see e.g. Van Eester and Koch 1998).

4. The case of rapidly varying Θ

Adopting (22) and the results of the previous section, the dielectric response W of a toroidal plasma to an RF perturbation can be computed when weak decorrelation of particles and waves is assumed. As such, the detailed relation between this expression and more familiar ones based on straight magnetic field lines is not immediately clear. In this section, the link will be established, but it will be shown that it relies on a number of assumptions that are not trivially satisfied.

4.1. General preliminary remarks

For each m_b of the sum on the bounce spectrum in (22), the Fourier amplitudes $\mathbf{F}^* \cdot \mathbf{v}_{\mathbf{m}}$ and $\mathbf{E} \cdot \mathbf{v}_{\mathbf{m}}$ have to be evaluated. Since the quantities $\mathbf{F}$ and $\mathbf{E}$ depend on the poloidal angle θ, each component $\mathbf{F}^* \cdot \mathbf{v}_{\mathbf{m}}$ or $\mathbf{E} \cdot \mathbf{v}_{\mathbf{m}}$ is actually a sum over the full poloidal spectrum, and thus W contains the triple sum $\sum_{m_b} \sum_m \sum_{m'}$ (where m_b is the bounce mode number, m is the poloidal mode number of $\mathbf{E}$, and m' is that of $\mathbf{F}$), which will henceforth be abbreviated as $\tilde{\Sigma}$. The second derivative of the phase Θ,

$$\Theta''_m = \omega_b^{-2} \ddot{\Theta} = \omega_b^{-2} \left(k_{\parallel m} \frac{v_\perp^2}{2 v_\parallel} - \frac{n v_\parallel \cos\tilde{\alpha}}{R_{gc}} + m_g \Omega \right) \frac{\dot{R}_{gc}}{R_{gc}}, \tag{24}$$

https://doi.org/10.1017/S0022377898007016 Published online by Cambridge University Press

is independent of m_b. When $m_g \neq 0$, it is large, and one can find from the stationary-phase condition that

$$\delta_{m_b} = \Theta'' \, \delta\Phi_{b,SPP}, \tag{25a}$$

and so $\Phi_{b,SPP}$ varies only slightly when going from m_b to m_b+1. The sum over the m_b spectrum can thus be recast into an integral over all possible positions of the stationary phase point, *provided* that the integrand itself varies slowly when going from m_b to m_b+1. Although Θ itself is rapidly varying as a function of m_b, the individual contributions to the bounce spectrum of the dielectric response can vary slowly. Since, for each m_b, several stationary-phase points exist for a given poloidal mode number, one should account for all cross-couplings when evaluating the dielectric response (which is the product of the Fourier amplitudes of $\mathbf{F}^* \cdot \mathbf{v_m}$ and $\mathbf{E} \cdot \mathbf{v_m}$). Aside from the replacement of the sum by an integral for a 'reference' stationary-phase point of the mode number m, all cross-coupling contributions from all stationary-phase points of m' belonging to the same m_b must be included. The result is

$$\sum_{m_b} \to \int_0^{2\pi} d\Phi_{b,SPP} \, |\Theta''_m| \sum_{SPP_{m'}}, \tag{25b}$$

where a subscript m has been attached to Θ to stress that it is evaluated for a given poloidal number m of the electric field.

The substitution (25*b*) makes apparent that the sum on the bounce spectrum is equivalent to the *bounce average* commonly appearing in RF diffusion operators used in Fokker–Planck computations. As has just been mentioned, the partial dielectric response integrand needs to be sufficiently slowly varying for this substitution to be justified. When modelling RF heating in a tokamak in the weak-decorrelation limit, a subtlety related to the bounce time scale emerges. Indeed, looking at the expression (10) for the dielectric response, or at its equivalent (22) after using the stationary-phase condition (21), the factor

$$\frac{1}{\mathbf{m} \cdot \boldsymbol{\omega} - \omega} = \frac{1}{m\dot{\theta}_{gc} + n\dot{}_{gc} + m_g \dot{\phi} - \omega}$$

is not a slowly varying function at all when its denominator goes through zero. Invoking the usual weak-decorrelation causality recipe, which consists in replacing ω by $\omega + i\nu$ (equivalent to adding an attenuation factor $e^{\nu t}$ to the integrand of (3)) and letting $\nu/\omega \to 0^+$ when evaluating the absorbed power, does not solve the problem but, quite on the contrary, makes it even more apparent: rather than a smooth slowly varying function, the power-density integrand then contains a delta function! To guarantee a sufficiently slowly varying integrand, the delta function has to be replaced by a function that varies slowly as a function of the bounce mode m_b. The simplest way to accomplish this is to slightly alter the usual causality recipe. The first step is kept, i.e. the resonant denominator is removed by substituting $\omega + i\nu$ for ω:

$$\frac{1}{\mathbf{m} \cdot \boldsymbol{\omega} - \omega} \to \frac{1}{\omega_b} \frac{m_b - m_{b\,\mathrm{res}} + i\nu/\omega_b}{(m_b - m_b\,\mathrm{res})^2 + (\nu/\omega_b)^2} = \mathscr{R}(m_b),$$

with

$$m_{b\,\mathrm{res}} = \frac{\omega - n\omega_d - m_g \omega_g}{\omega_b}.$$

https://doi.org/10.1017/S0022377898007016 Published online by Cambridge University Press

Rather than subsequently taking the limit $\nu \to 0^+$, which yields *rapid* variations of $\mathscr{R}(m_b)$ when $m_b \approx m_{b\mathrm{res}}$, ν/ω_b is assumed to be *large*. The real part of the function $\mathscr{R}$ then replaces the resonance by a quasiresonance, while its imaginary part is a localized but smooth function centred on $m_{b\mathrm{res}}$ replacing the delta function. Combining both conditions on ν, one gets

$$\omega_b \ll \nu \ll \omega, \tag{25c}$$

which requires the decorrelation process to take place on a time scale in between that of the cyclotron and bounce time scales. The term 'weak decorrelation' thus inadequately characterizes the regime for which the substitution (25*b*) is justified: the decorrelation is weak on the cyclotron but strong on the bounce time scale. In simple straight-magnetic-field-line quasi-uniform plasma models, the bounce spectrum is absent and the first of the above inequalities falls so that the only condition the decorrelation frequency ν has to satisfy is that it should be small compared with the cyclotron time scale. The decorrelation frequency can in that case simply be interpreted as the collision frequency, whose magnitude is vanishingly small compared with the RF driver frequency. In toroidal geometry, the guiding-centre orbits are closed poloidally, and so the supplementary bounce time scale complicates the problem. Since the collision frequency commonly is significantly shorter than the bounce time, this forces one to look for more efficient decorrelation mechanisms in order to validate the substitution (25*b*) that leads to local resonances on the particle's orbits. Several authors have examined such more sophisticated decorrelation mechanisms, and have concluded that sufficiently efficient decorrelation mechanisms exist (see e.g. Kasilov *et al*. (1990) for decorrelation due to the inhomogeneity of the static magnetic field and Bécoulet *et al*. (1994) for decorrelation due to the presence of sufficiently large electric fields). In the case where such a mechanism does not exist, the parameter ν/ω_b is not large, and local resonances are gradually replaced by global ones. When ν/ω_b is of order 1, the effect of constructive/destructive interference of successive resonance crossings can clearly be recognized on the power density (see Van Eester *et al*. 1996). When ν/ω_b is small, a different regime characterized by

$$\nu \ll \omega_b \ll \omega \tag{25d}$$

is identified. Not only is the substitution of the bounce sum by an integral then not justified, but also the existence of a resonant bounce mode is not certain, since the width of $\mathrm{Im}\{\mathscr{R}(m_b)\}$ is then much smaller than the distance between two neighbouring bounce modes, so that absorption is only guaranteed if $m_{b\mathrm{res}}$ is sufficiently close to an integer that lies inside the bounce spectrum. The vanishing of the absorption in the limit $\nu/\omega_b \to 0^+$ is the signature of the so-called superadiabatic regime. Whereas the simple straight-magnetic-field-line quasi-uniform plasma models predict the absorbed power density to be insensitive to the actual value of ν as long as it is sufficiently small, the closed poloidal orbits put a lower limit on the smallness of ν.

The above inequalities decide on a global justification of the substitution (25*b*). Independent of the actual value of ν, the substitution can also locally be unjustified. In the expression for Θ''_m, the cyclotron term dominates the others when $m_g \neq 0$, and thus Θ''_m changes sign very close to (trapped particles) or at (passing particles) the turning points where $\dot{R}_{gc} = 0$. Near these points, the stationary-phase points are not closely spaced, and the substitution $\delta m_b \to$

https://doi.org/10.1017/S0022377898007016 Published online by Cambridge University Press

$\Theta''\delta\Phi_{b,SPP}$ from a discrete to a continuous variable introduces artefacts into the model. Moreover, the m_b spectra of two differing poloidal mode numbers are displaced with respect to one another (see the discussion later). Because only the m_b that contribute to both spectra should be accounted for, part of the bounce-average interval $[0, 2\pi]$ may have to be excluded.

For a given m_b, the stationary-phase points corresponding to m and m' are generally distinct, but the dielectric response W, a double sum of the full poloidal spectrum, is symmetric in (m, m'). It can be written as

$$\mathsf{W} = -\omega\mu_0\left(\frac{2\pi q}{m}\right)^2 \int dr_{gc}\frac{\partial\Psi_{gc}}{\partial r_{gc}}\int d\varepsilon\int d\mu\frac{1}{\omega_b}\sum_n\sum_m\sum_{m'}\sum_{m_g}\int_0^{2\pi} d\Phi_{b,SPP}|\Theta''_m| \times \sum_{SPP_{m'}} \mathscr{N}^{\,m}_{m'}\frac{1}{m\dot{\theta}_{gc}+n\dot{}_{gc}+m_g\dot{\theta}-\omega}, \tag{26a}$$

where

$$\mathscr{N}^{\,m}_{m'} = \frac{1}{2\pi}\mathscr{L}_{m_g,m'}(\mathbf{F})*\left[\frac{\partial F_0}{\partial\varepsilon}\mathscr{L}_{m_g,m}(\mathbf{E})+\frac{\partial F_0}{\partial\mu}\hat{\mathscr{L}}_{m_g,m}(\mathbf{E})\right] \times\frac{\exp\{-i[\Theta_{m'}-\frac{1}{2}\arg(\Theta''_{m'})]\}}{|\Theta'_{m'}|^{1/2}}\frac{\exp\{i[\Theta_m-\frac{1}{2}\arg(\Theta''_m)]\}}{|\Theta''_m|^{1/2}}, \tag{26b}$$

$$\left.\begin{aligned}\mathscr{L}_{m_g,m}(\mathbf{G}) &= \tilde{\mathscr{L}}_{m_g,m}(\mathbf{G})+v_\parallel\exp(-im_g\psi)J_{-m_g}(\chi)G_\parallel,\\ \tilde{\mathscr{L}}_{m_g,m}(\mathbf{G}) &= \tfrac{1}{2}v_\perp\{\exp[i(1-m_g)\psi]J_{1-m_g}(\chi)G_- +\exp[-i(1+m_g)\psi]J_{-1-m_g}(\chi)G_+\},\\ \hat{\mathscr{L}}_{m_g,m}(\mathbf{G}) &= \frac{1}{B_0}\tilde{\mathscr{L}}_{m_g,m}(\mathbf{G}).\end{aligned}\right\} \tag{26c}$$

The slowly varying quantities $v_\perp, v_\parallel, \ldots$, have to be evaluated at the stationary-phase angles.

The individual contributions to the above sum contain factors that, except for the factor $\exp[i(\Theta_m-\Theta_{m'})]$, vary slowly with m_b. When this new phase factor does not exhibit large variations, fast Fourier transforms can, just as for the earlier evaluation of the individual bounce amplitudes, be used to evaluate the integrals. When $m_g \neq 0$, the individual contributions Θ_m and $\Theta_{m'}$ to the new phase are large owing to the cyclotron contributions, and result in rapidly varying exponential factors $\exp(i\Theta_m)$ and $\exp(-i\Theta_{m'})$. In the case where the substitution (25*b*) is justified, and provided that the *product* of the individual rapidly varying factors is a rapidly varying function as well, the stationary-phase method can be used to evaluate the new bounce integral. Note, however, that conflicting assumptions are needed for the stationary-phase method to be applicable for this second step: *if* the substitution (25*b*) is justified, the factor $\exp[i(\Theta_m-\Theta_{m'})]$ is sufficiently *slowly* varying as a function of m_b to enable a good sampling of the oscillations. Consequently, the stationary-phase method, which relies on *rapid* phase variations, is not trivially applicable. That the stationary-phase points of the new phase are the points where the substitution (25*b*) is most questionable can be shown analytically: indeed, the relative phase is $\tilde{\Theta}_{m,m'} = \Theta_m - \Theta_{m'}$, with $\Theta_{m,m'}$ given by (16) after elimination of m_b using (19):

$$\Theta_m = -\left[\sum_{l=1}^{\infty} l\xi_{l,m_g}\cos(l\Phi_{b_{m_1}})\right]\Phi_{b_{m_1}}+\sum_{l=1}^{\infty}\xi_{l,m_g}\sin(l\Phi_{b_{m_1}}).$$

https://doi.org/10.1017/S0022377898007016 Published online by Cambridge University Press

It is readily found from this expression that

$$\Theta'_m = -\Theta''_m \Phi_{b_m},$$

with $' = d/d\Phi_{b_m}$. As $d\Phi_{b_{m'}}/d\Phi_{b_m} = \Theta''_m/\Theta''_{m'}$, the new stationary-phase condition is

$$\tilde{\Theta}'_{m,m'} = -\Theta''_m \Phi_{b_m} + \frac{\Theta''_m}{\Theta''_{m'}} \Theta''_{m'} \Phi_{b_{m'}} = -\Theta''_m(\Phi_{b_m} - \Phi_{b_{m'}}) = 0. \tag{27}$$

Aside from the trivial case where the stationary-phase points coincide and the relative phase is zero, the stationary-phase points satisfy the turning-point condition $\Theta'' = 0$; the corresponding second derivative is

$$\tilde{\Theta}''_{m,m'} = -\Theta'''_m(\Phi_{b_m} - \Phi_{b_{m'}}) - \Theta''_m\left(1 - \frac{\Theta''_m}{\Theta''_{m'}}\right).$$

The role of the turning points as the stationary-phase of the new phase could be anticipated: near the turning points on the guiding centre's trajectory, the second derivative of the phase vanishes, since $\ddot{\Theta} \propto \dot{R}_{gc}$ and $\dot{R}_{gc}$ goes through zero there *independently* of the specific value of m. Because the derivative of the cyclotron frequency vanishes, the phase varies slowly very close to the turning point. The need for a more refined model near the stationary-phase points has already been mentioned. As far as the computation of the RF-induced time derivative of the energy or the magnetic moment are concerned, this refinement is straightforward (replacement of (17) by (20)). Analytical refinement of the practical evaluation of the global dielectric response of the whole bounce spectrum is less trivial, and falls outside the scope of the present paper.

To get a better feeling of the variations of the relative phase $\tilde{\Theta}_{m,m'}$, we take a closer look at it. Introducing the notation

$$\xi_{l,m,m_g} = \xi_+ + \xi_-, \qquad \xi_{l,m,m_g} = \xi_+ - \xi_-, \tag{28a}$$

$$\Phi_+ = \tfrac{1}{2}(\Phi_{b_m} + \Phi_{b_{m'}}), \qquad \Phi_- = \tfrac{1}{2}(\Phi_{b_m} - \Phi_{b_{m'}}) \tag{28b}$$

$$\xi_+ = \xi_{l,(m+m')/2,m_g} = \frac{\frac{1}{2}(m+m')\,\mathfrak{P}_l + n\mathfrak{T}_l + m_g\,\mathfrak{F}_l}{l\omega_b}, \qquad \xi_- = \frac{\frac{1}{2}(m-m')\,\mathfrak{P}_l}{l\omega_b}, \tag{28c}$$

this phase can then be written as

$$\begin{aligned}\tilde{\Theta}_{m,m'} = 2\Bigg\{ &\sum_{l=1}^{\infty} l\xi_+[\Phi_+ \sin(l\Phi_+)\sin(l\Phi_-) - \Phi_- \cos(l\Phi_+)\cos(l\Phi_-)] \\ &+ \sum_{l=1}^{\infty} l\xi_-[\Phi_- \sin(l\Phi_+)\sin(l\Phi_-) - \Phi_+ \cos(l\Phi_+)\cos(l\Phi_-)] \\ &+ \sum_{l=1}^{\infty} [\xi_+ \cos(l\Phi_+)\sin(l\Phi_-) + \xi_- \sin(l\Phi_+)\cos(l\Phi_-)]\Bigg\} \\ &- \tfrac{1}{2}\arg(\Theta''_m) + \tfrac{1}{2}\arg(\Theta''_{m'}) = -\tilde{\Theta}_{m',m}.\end{aligned} \tag{29}$$

Because the ξ_- terms no longer have a cyclotron contribution, they are much smaller than the ξ_+ terms, and their contribution in general does not cause large phase variations. For the stationary-phase method to be valid, the terms proportional to ξ_+ then need to be large. This is only the case when Φ_- is globally not too small (although it may go through zero at the stationary-phase point). It is interesting to note that Φ_- is larger when m and m' are further

https://doi.org/10.1017/S0022377898007016 Published online by Cambridge University Press

Table 1. Bounce spectrum of the phase Θ for a passing 2 keV H close to the trapped/passing edge at $r_{gc} = 1.2$ m; $\varepsilon = 3.2 \times 10^{-16}$ J, $\mu = 6.1 \times 10^{-17}$ J T^{-1} and $(m, m', n, m_g) = (-5, 5, 10, -1)$

l	ξ_l for $m = -5$	ξ_l for $m' = 5$
1	-3.092×10^{3}	-3.084×10^{3}
2	-3.104×10^{2}	-3.103×10^{2}
3	$+3.234 \times 10^{1}$	$+3.224 \times 10^{1}$
4	$+1.457 \times 10^{1}$	$+1.457 \times 10^{1}$
5	-1.232×10^{-1}	-1.199×10^{-1}
6	-8.289×10^{-1}	-8.282×10^{-1}
7	-8.657×10^{-2}	-8.668×10^{-2}
8	$+3.974 \times 10^{-2}$	$+3.970 \times 10^{-2}$
9	$+6.830 \times 10^{-3}$	$+6.837 \times 10^{-3}$
10	-4.583×10^{-3}	-4.576×10^{-3}

apart, and thus the applicability of the stationary-phase method is more justified when the poloidal mode numbers are well separated. Aside from the case just discussed, (27) also suggests that the opposite case, $\Phi_{b_m} = \Phi_{b_{m'}}$ (which requires $m = m'$), also gives rise to stationary-phase points. In this case, however, the phase $\tilde{\Theta}_{m,m'}$ is identically zero, and the integrand only varies as a result of the slowly varying quantities $v_\perp, v_\parallel, \ldots$. The latter case, as well as the case $m \approx m'$, can be dealt with using fast Fourier transforms, or taking advantage of the closeness of the stationary-phase points, as will be explained in Sec. 4.3.

4.2. Numerical evaluation of the stationary-phase angles

Before proceeding further in the analytical treatment of the dielectric response in the case where the phase factor (16) is rapidly varying, a qualitative feeling of where the stationary-phase angles corresponding to different poloidal mode numbers lie, and what the factor $\exp(i\tilde{\Theta}_{m,m'})$ appearing in the dielectric response function W looks like, is now provided by giving a few numerical examples. The parameters are typical for JET, but a circular cross-section has been assumed: $B_0 = 3.1$ T, $R_0 = 3$ m, $a_p = 1.25$ m and $I_p(a_p) = 4$ MA.

The first example corresponds to a passing 2 keV H ion ($\varepsilon = 3.2 \times 10^{-16}$ J) close to the trapped/passing boundary and circulating on the surface $r_{gc} = 1.2$ m. For the adopted parameters, the trapped/passing edge is at $\mu = 6.19 \times 10^{-17}$ J T^{-1}; the magnetic moment was taken to be $\mu = 6.1 \times 10^{-17}$ J T^{-1}. The $m_g = -1$ gyro mode number, relevant for heating at the fundamental cyclotron frequency, is chosen, and the poloidal mode numbers of the electric field and the test function are -5 and 5 respectively. The toroidal mode number is 10.

For these parameters, the magnitude of the velocity is 6.19×10^5 m s^{-1}, the maximum (minimum) parallel velocity is 4.71×10^5 (7.61×10^4) m s^{-1} and the maximum (minimum) perpendicular velocity is 6.14×10^5 (4.02×10^5) m s^{-1}. The bounce frequency is 4.71×10^4 Hz. Given the fixed velocity and the imposed magnetic field strength variation on the considered magnetic surface, only a restricted interval of constant values of the magnetic moment is accessible. The maximal magnetic moment for the given energy is 1.45×10^{-16} J T^{-1}. Table 1 shows the first Fourier amplitudes of the periodic part

https://doi.org/10.1017/S0022377898007016 Published online by Cambridge University Press

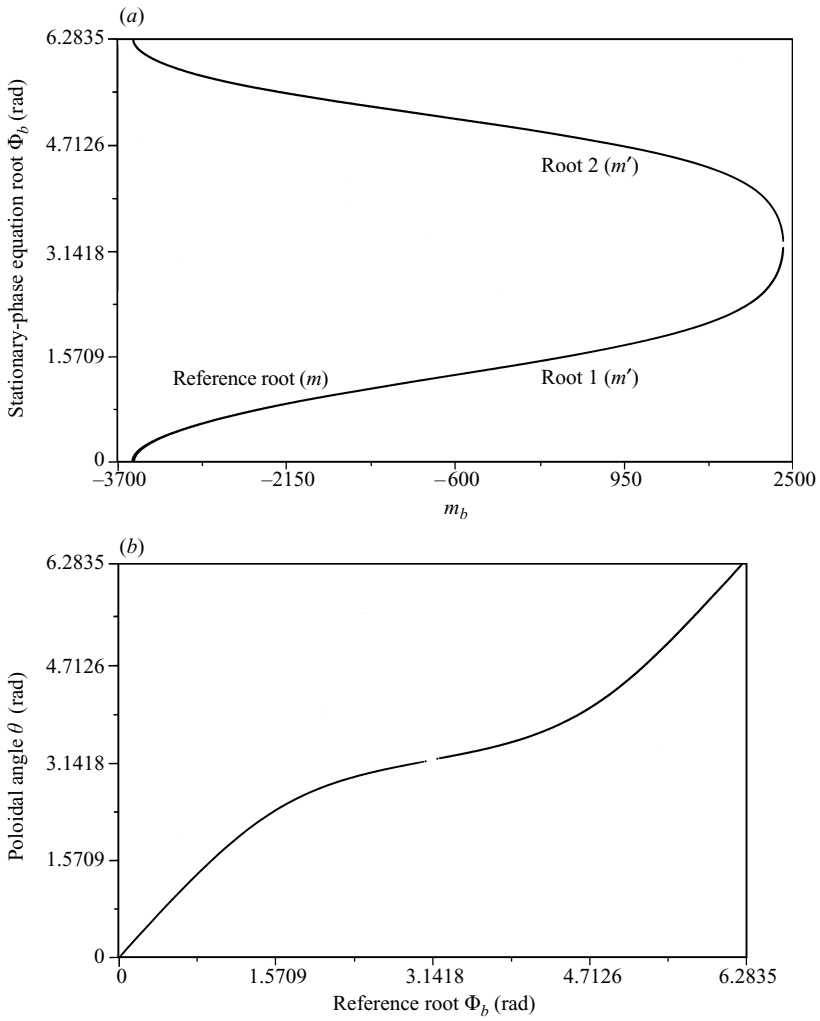


Figure 1. For legend see facing page.

of the phase Θ (see (B 2) and (16)). The computations in this section were done using all terms up to $l = 23$; the table shows, however, that keeping the first few would have been sufficient for most purposes. The bounce spectrum for $m = -5$ runs from $m_b = -3568$ to $m_b = 2424$, and that for $m' = 5$ from $m_b = -3551$ to $m_b = 2427$. Figure 1 (a) shows the stationary-phase positions as a function of the bounce mode number. Owing to the up–down symmetry of the orbits, an up–down symmetry of the bounce modes results. For each bounce mode number m_b and poloidal mode number m or m', two stationary-phase points exist. Because of the width of the bounce spectrum, the substitution (25b) of the sum on the bounce modes by the bounce integral over the associated stationary-phase points is well justified, except close to the turning points (see later for a more detailed discussion on this point): although each stationary-phase position was indicated by a dot, the figure represents a virtually continuous line. The stationary-phase points for both poloidal mode numbers are also barely distinguishable. Figure 1 (b) depicts the relation

https://doi.org/10.1017/S0022377898007016 Published online by Cambridge University Press

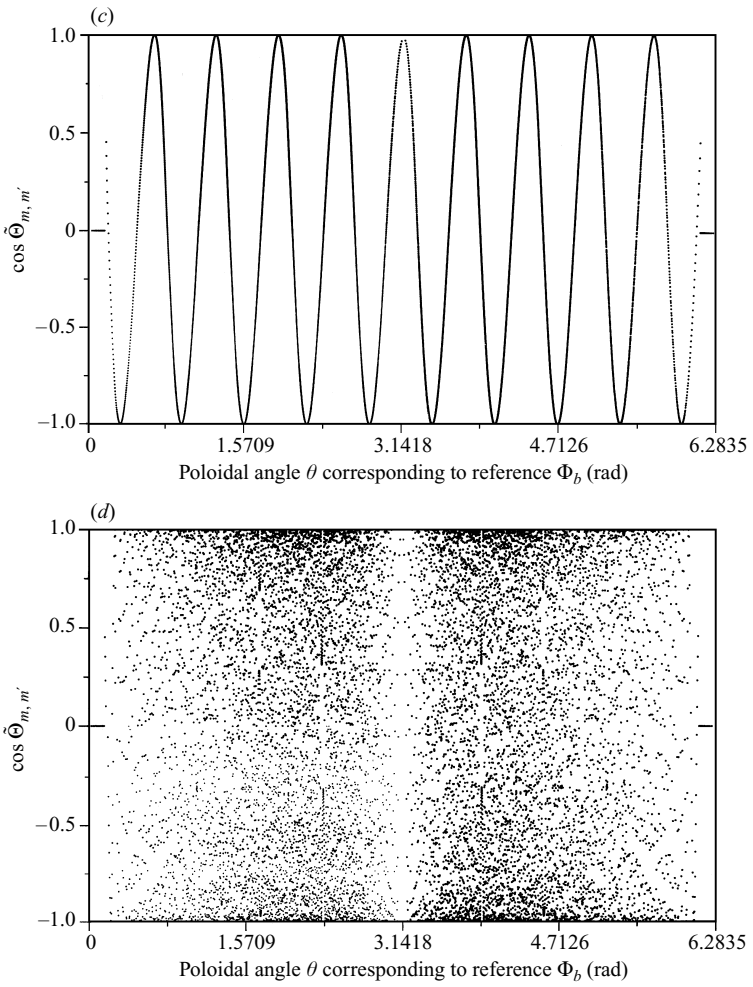


Figure 1. Passing 2 keV H at $r_{gc} = 1.2$ m close to the trapped/passing edge ($\mu_{\text{edge}} = 6.19 \times 10^{-17}$ J T^{-1}); $\varepsilon = 3.2 \times 10^{-16}$ J, $\mu = 6.1 \times 10^{-17}$ J T^{-1}, $m = -5$, $m' = 5$, $n = 10$, $m_g = -1$: (*a*) stationary-phase angles as a function of the bounce mode m_b; (*b*) relation between the usual poloidal angle and the angle $\Phi_b = \omega_b t$; (*c*) $\cos\tilde{\Theta}_{m,m'}$ for 'close' roots; (*d*) $\cos\tilde{\Theta}_{m,m'}$ for 'far' roots.

between the usual poloidal angle and the Φ_b stationary-phase angle. Remembering that Φ_b is proportional to the time spent by a guiding centre to reach a given poloidal position, the deceleration of the passing particle near the HFS crossing through the midplane is clearly visible. The real part of the relative phase factor $\exp(i\tilde{\Theta}_{m,m'})$ for the reference root and the nearby root of the mode number $m' = 5$ is depicted in Fig. 1(*c*). It shows a nearly harmonic oscillation with an effective mode number $m - m'$. The real part of the factor $\exp(i\tilde{\Theta}_{m,m'})$ for the reference root and the far root of the mode number $m' = 5$ is depicted in Fig. 1(*d*). In contrast to Fig. 1(*c*), we now seemingly observe a nearly arbitrary value of $\exp(i\tilde{\Theta}_{m,m'})$. This very different behaviour is easily explained by glancing at (28) and (29): remembering that the ξ_+ coefficients are large (see Table 1) because of the presence of the cyclotron variation term in

https://doi.org/10.1017/S0022377898007016 Published online by Cambridge University Press

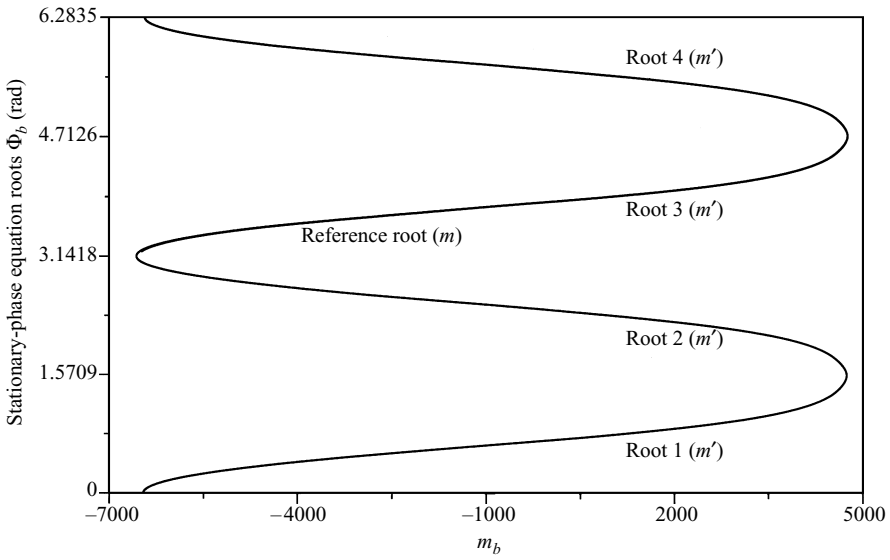


Figure 2. Stationary-phase angles for trapped 2 keV H near the trapped/passing edge. The parameters are as in fig. 1, except that $\mu = 6.3 \times 10^{-17}$ J T^{-1}.

Table 2. Bounce spectrum of the phase Θ for a trapped 2 keV H close to the trapped/passing edge at $r_{gc} = 1.2$ m; $\varepsilon = 3.2 \times 10^{-16}$ J, $\mu = 6.3 \times 10^{-17}$ J T^{-1} and $(m, m', n, m_g) = (-5, 5, 10, -1)$

l	ξ_l for $m = -5$	ξ_l for $m' = 5$
1	$+4.002 \times 10^{1}$	$+7.043 \times 10^{1}$
2	-2.906×10^{3}	-2.906×10^{3}
3	-2.824×10^{0}	-1.554×10^{0}
4	-2.436×10^{2}	-2.436×10^{2}
5	-8.841×10^{-1}	-1.003×10^{0}
6	$+3.324 \times 10^{1}$	$+3.324 \times 10^{1}$
7	$+6.120 \times 10^{-3}$	-3.775×10^{-2}
8	$+1.095 \times 10^{1}$	$+1.095 \times 10^{1}$
9	$+6.891 \times 10^{-2}$	$+8.024 \times 10^{-2}$
10	-9.608×10^{-1}	-9.608×10^{-1}

them, and realizing that $\Phi_- \approx 0$ and $\Phi_+ \approx \Phi_{b_m}$ for Fig. 1 (*c*), while $\Phi_+ \approx \pi$ and $\Phi_- \approx \Phi_{b_m}$ for Fig. 1 (*d*), the most rapidly varying terms are to a large extent eliminated in the former, while some of them remain in the latter case. The rapid variation of the factor $\exp(i\tilde{\Theta}_{m,m'})$ for 'far' roots of the stationary-phase condition equation has an important practical consequence: because small variations of the orbit parameters (ε or μ), although causing only small variations of the ξ_l and the stationary-phase positions Φ_b, cause variations of the order of a full period of the relative phase $\tilde{\Theta}_{m,m'}$, the contribution to the dielectric response of the 'far' roots after integration over velocity space (i.e. over many periods of $\tilde{\Theta}_{m,m'}$) is expected to be negligible compared with that of the 'near' roots.

For a trapped particle, the number of stationary-phase points doubles. Figure 2 depicts these points for a 2 keV trapped particle close to the

https://doi.org/10.1017/S0022377898007016 Published online by Cambridge University Press

Table 3. Bounce spectrum of the phase Θ for a deeply trapped 2 keV H at $r_{gc} = 1.2$ m; $\varepsilon = 3.2 \times 10^{-16}$ J, $\mu = 1.44 \times 10^{-16}$ J T^{-1} and $(m, m', n, m_g) = (-5, 5, 10, -1)$

l	ξ_l for $m = -5$	ξ_l for $m' = 5$
1	$+1.300 \times 10^{0}$	$+2.866 \times 10^{0}$
2	-4.500×10^{0}	-4.500×10^{1}
3	-7.075×10^{-3}	-1.485×10^{-2}
4	$+3.148 \times 10^{-2}$	$+3.148 \times 10^{-2}$
5	$+2.088 \times 10^{-3}$	$+4.585 \times 10^{-3}$
6	-8.049×10^{-3}	-8.049×10^{-3}
7	-1.006×10^{-3}	-2.211×10^{-3}
8	$+3.427 \times 10^{-3}$	$+3.427 \times 10^{-3}$
9	$+5.726 \times 10^{-4}$	$+1.259 \times 10^{-3}$
10	-1.855×10^{-3}	-1.855×10^{-3}

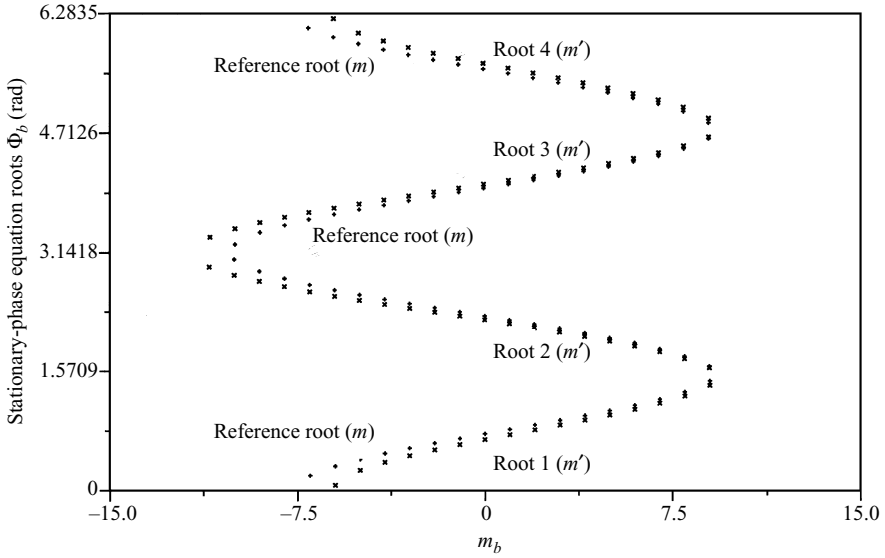


Figure 3. Stationary-phase positions for a deeply trapped 2 keV H. All parameters are as in Fig. 1, except that $\mu = 1.44 \times 10^{-17}$ J T^{-1} (the maximum μ for a 2 keV H at $r_{gc} = 1.2$ m is 1.45×10^{-16} J T^{-1}).

trapped/passing edge; the parameters are as before, except that $\mu = 6.30 \times 10^{-17}$ J T^{-1}. The maximum (minimum) parallel velocity is 4.65×10^{5} (0) m s^{-1} and the maximum (minimum) perpendicular velocity is 6.19×10^{5} (4.09×10^{5}) m s^{-1}. The bounce frequency is 2.44×10^{4} Hz and the banana tip is at $\theta = 2.91$ rad. The first Fourier amplitudes of the periodic part of the phase Θ are given in Table 2. The pair coefficients dominate the odd ones, reflecting the double periodicity superposed on the up–down symmetry of the trapped particles; the odd coefficients are due to the dependence of the phase Θ on the sign of $v_{\parallel}$. The width of the bounce spectrum has doubled: $-6543 \leqslant m_b \leqslant 4741$ for $m = -5$, and $-6576 \leqslant m_b \leqslant 4741$ for $m = 5$. As in Fig. 1, the individual dots cannot be distinguished, and the points for the two poloidal mode numbers virtually coincide.

https://doi.org/10.1017/S0022377898007016 Published online by Cambridge University Press

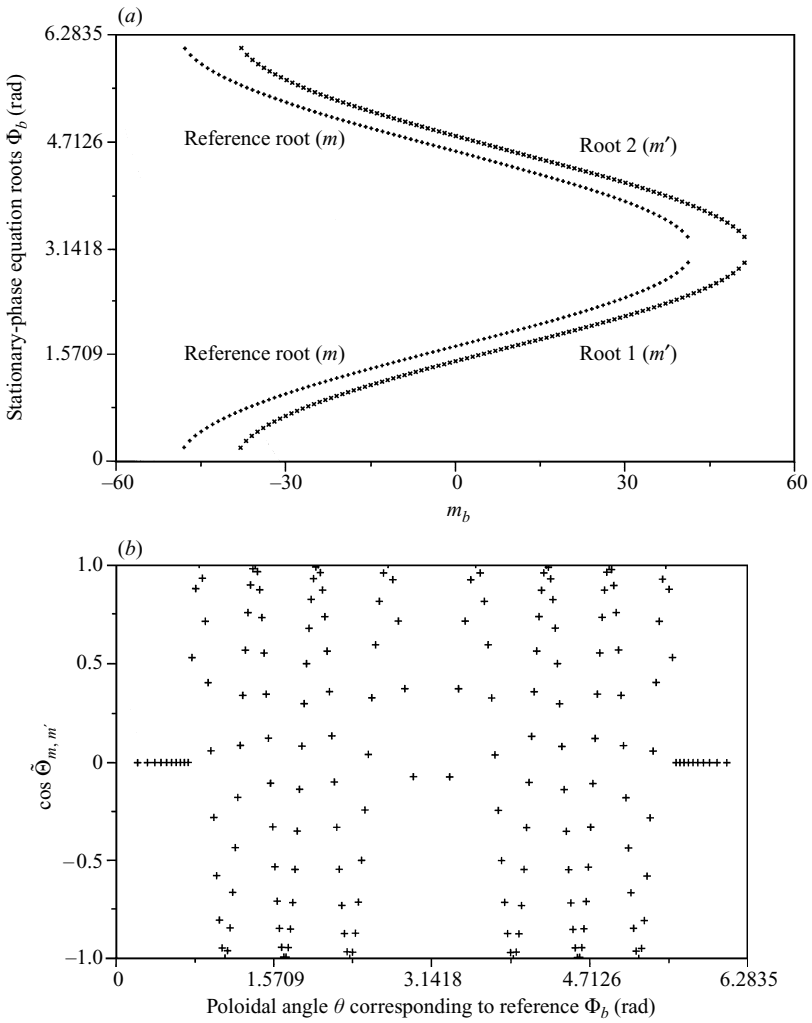


Figure 4. Stationary-phase positions (a) and $\cos\tilde{\Theta}_{m,m'}$ (b) for a well-passing 2 keV H at $r_{ge} = 0.2$ m. All parameters are as in Fig. 1, except that $\mu = 1.44 \times 10^{-18}$ J T^{-1}.

Along deeply trapped orbits that cover only a small portion of the magnetic surface, the variations of $v_\parallel$, $v_\perp$ and Ω are relatively small and the bounce spectrum contains a smaller number of significant terms. For $\mu = 1.44 \times 10^{-16}$ J T^{-1} (and all parameters as before), the banana tip is at $\theta = 0.16$ rad, the perpendicular velocity varies between 6.19×10^5 m s^{-1} and 6.18×10^5 m s^{-1}, while the parallel velocity varies between 3.7×10^4 m s^{-1} and 0. The bounce frequency is 4.18×10^4 Hz. The first few Fourier harmonics of the periodic part of the rapidly varying phase are given in Table 3.

The bounce spectrum for $m = -5$ contains only 21 terms ($-10 \leqslant m_b \leqslant 10$); that for $m' = 5$ has one more ($-11 \leqslant m_b \leqslant 10$). As can be seen in Fig. 3, the stationary-phase positions for the various m_b are more widely spaced than was the case for the particles near the trapped/passing edge; the spacing is widest near the turning points (banana tips and the crossing of the midplane). This

https://doi.org/10.1017/S0022377898007016 Published online by Cambridge University Press

demonstrates numerically that the replacement (25*b*) of the sum on the bounce modes by a bounce integral is less justified for this orbit than it was for the particles near the trapped/passing edge, especially near the turning points. Since the orbit covers only a small fraction of the poloidal circumference, the factor $\exp(i\tilde{\Theta}_{m,m'})$ is only well sampled if the poloidal mode numbers are not too far apart. The figure also shows that the validity of the substitution is questionable for another reason: since the bounce spectra of the two poloidal modes do not overlap exactly, no 'near' root exists for the $m' = +5$ mode when it already exists for the $m = -5$ mode. In practical terms, this means that the dielectric response is only nonzero on that part of the poloidal circumference for which stationary-phase positions exist for both modes, and so replacing of the bounce sum by a bounce integral on the full bounce is not justified. This wide spacing as well as clipping or part of the bounce integral near the turning points is not solely observed for the well-trapped particles: it could already be recognized in Fig. 1(*c*).

Because the width of the bounce spectrum is linked to the relative variation (of e.g. Ω) on the orbit, one equally expects this poorer sampling on magnetic surfaces close to the magnetic axis. This is indeed obvious when looking at Fig. 4(*a*), in which the stationary-phase angles for a well-passing 2 keV H orbit at $r_{gc} = 0.2$ are depicted. The discreteness of the spectrum as well as the separation of the stationary-phase angle of the two poloidal modes for a given bounce mode are clearly visible. In about one-quarter of the total poloidal trajectory, the dielectric response is zero (see Fig. 4*b*). It can furthermore be recognized that the factor $\exp(i\tilde{\Theta}_{m,m'})$ no longer behaves as a pure harmonic oscillation with effective poloidal mode number $m - m'$: the oscillation has an increasingly longer wavelength towards the HFS turning point ($\theta = \pi$).

Another effect that separates the stationary-phase points for a given pair of poloidal modes is the magnitude of the 'Doppler-shift' contribution $m\dot{\theta}_{gc} + n\dot{\zeta}_{gc} (= k_\parallel v_\parallel)$ on the left-hand side of the stationary-phase condition (21). For a given type of trajectory and machine settings, this factor is enhanced by considering more-energetic particles or by considering more widely separated poloidal modes. Figure 5(*a*) depicts the stationary-phase angles for a 2 keV H at $r_{gc} = 1.2$ m and all parameters as before, while Fig. 5(*c*) represents the same case for a 50 keV proton, and Fig. 5(*e*), finally, depicts the result for a 50 keV proton with $m = -60$ and $m' = +60$. It can clearly be seen that the roots of (21) for a given m_b are increasingly more widely spaced on going from Fig. 5(*a*) to 5(*e*). Again, the bounce spectrum is relatively wide for most orbits, and so the substitution (25*b*) is, at first sight, justified away from the turning points. A gradually worse sampling of $\exp(i\tilde{\Theta}_{m,m'})$ can be observed on going from Fig. 5(*b*) to 5(*d*) and finally to 5(*f*). For $(m, m') = (-60, 60)$, the function $\exp(i\tilde{\Theta}_{m,m'})$ is so rapidly oscillating that it appears to be a random value. As the inset in the tiny domain ($3.14\,\text{rad} < \theta < 3.5\,\text{rad}$) shows, the function is well behaved but poorly sampled by the individual modes of the bounce spectrum.

That the roots of (21) can be very far apart is demonstrated in Fig. 6, which shows the stationary-phase angles for a deeply trapped 50 keV H orbit at $r_{gc} = 1.2$ m for poloidal mode numbers $m = -60$, $m' = 60$ and toroidal mode number $n = 40$. Not only do the two bounce spectra overlap but on a small number of bounce modes only, two rather than the usual four roots exist for the m' mode. The asymmetry of the forward and backward legs of the trapped particle has

https://doi.org/10.1017/S0022377898007016 Published online by Cambridge University Press

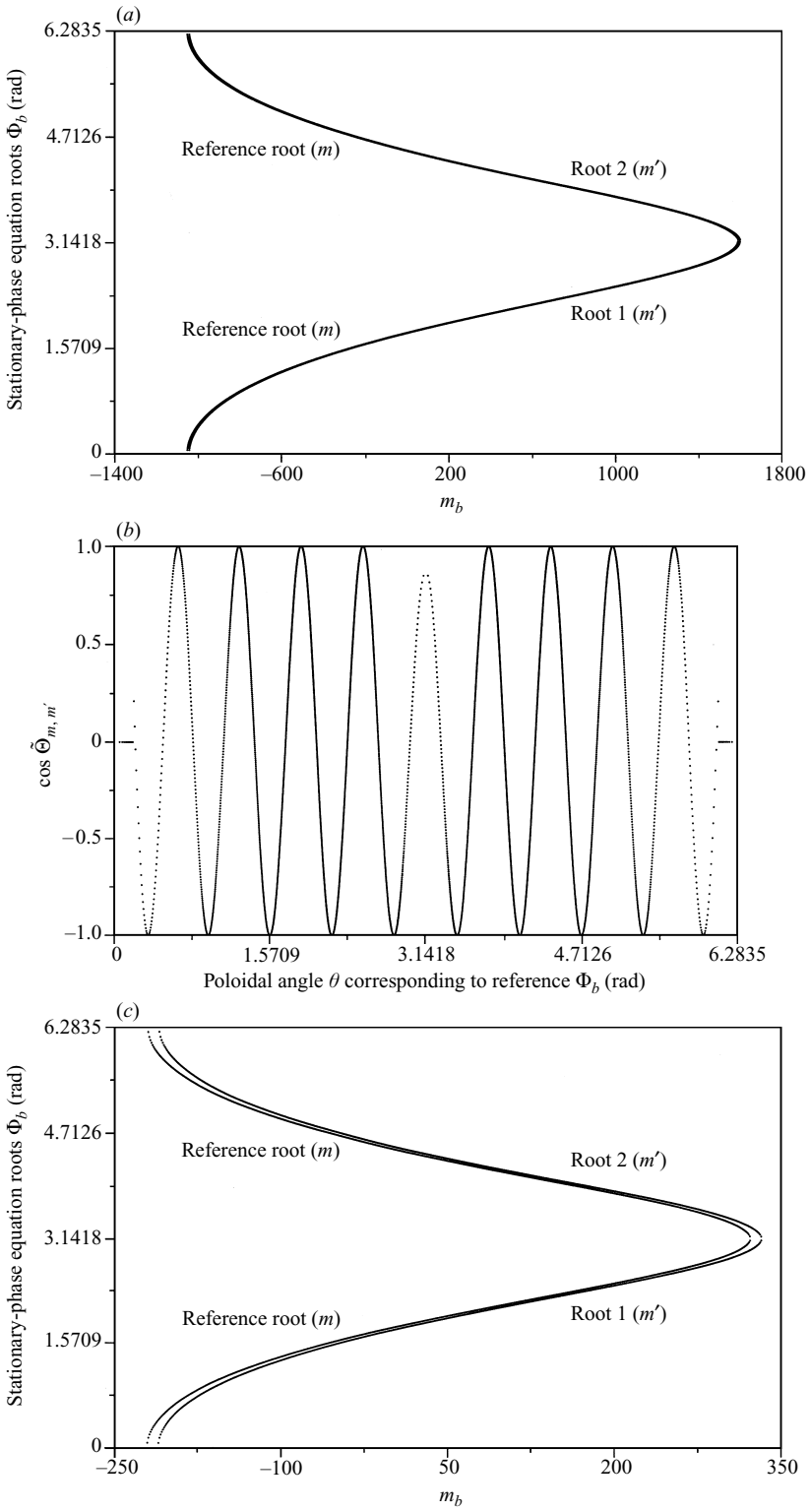


Figure 5. For legend see facing page.

https://doi.org/10.1017/S0022377898007016 Published online by Cambridge University Press

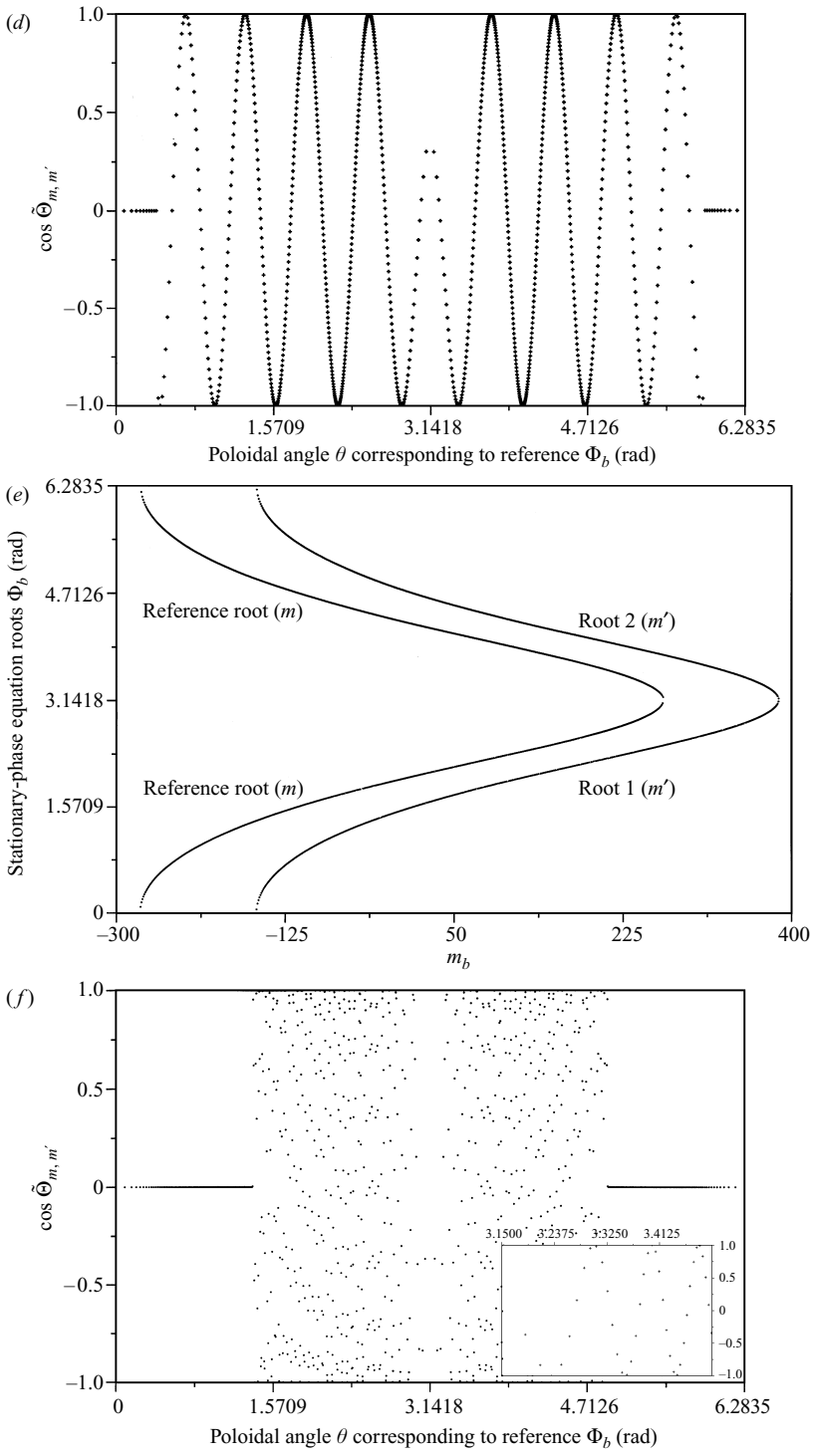


Figure 5. Stationary-phase positions (a, c, e) and cosine of the relative phase $\tilde{\Theta}_{m,m'}$ (b, d, f) for a well-passing H at $r_{gc} = 1.2$ m. All parameters are as in Fig. 1, except as follows: (a, b) $\varepsilon = 3.2 \times 10^{-16}$ J (2 keV), $\mu = 1.44 \times 10^{-18}$ J T^{-1}, $m = -5$, $m' = 5$; (c, d) $\varepsilon = 8.0 \times 10^{-15}$ J (50 keV), $\mu = 3.6 \times 10^{-17}$ J T^{-1}, $m = -5$, $m' = 5$; (e, f) $\varepsilon = 8.0 \times 10^{-15}$ J (50 keV), $\mu = 3.6 \times 10^{-17}$ J T^{-1}, $m = -60$, $m' = 60$. The inset in (f) shows the sampling of $\cos \tilde{\Theta}_{m,m'}$ over a small fraction of the orbit (3.15 rad $< \theta <$ 3.5 rad).

https://doi.org/10.1017/S0022377898007016 Published online by Cambridge University Press

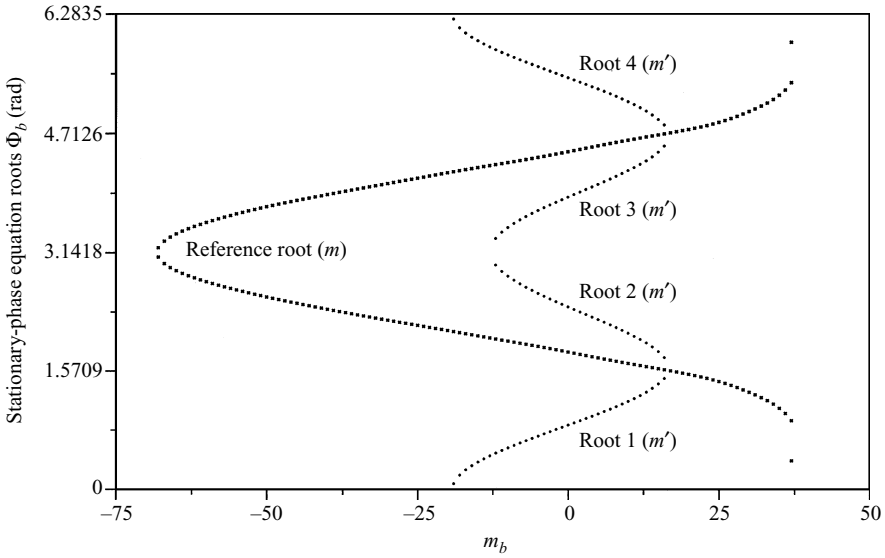


Figure 6. Stationary-phase positions for a deeply trapped H at $r_{gc} = 1.2$ m. All parameters are as in Fig. 1, except that $\varepsilon = 8.0 \times 10^{-15}$ J (50 keV), $\mu = 3.5 \times 10^{-15}$ J T^{-1}, $m = -60$, $m' = 60$ and $n = 40$.

been observed before, but it is striking in this example. Figure 7 shows how this asymmetry can systematically be decreased: starting from the totally asymmetric spectrum in Fig. 6, the two extra root branches are recovered by reducing the poloidal mode number ($m = m' = 10$ and $n = 40$; Fig. 7*a*) or the toroidal mode number ($m = m' = 10$ and $n = 0$; Fig. 7*b*). A virtually symmetric spectrum is found in absence of the Doppler shift ($m = m' = 10$ and $n = 0$; Fig. 7*c*).

In this section, it has been demonstrated numerically that the replacement of the sum on the bounce spectrum by a bounce integral is not trivially justified if B_0 is nearly homogeneous along the orbit, as is the case for deeply trapped particles and for particles near the magnetic axis. Whether or not the sum on the bounce modes can be replaced by a bounce integral depends critically on the sensitivity of the partial dielectric response to m_b. As long as a few m_b lie within each oscillation of the factor $\exp(i\tilde{\Theta}_{m,m'})$ (the most rapidly varying factor in the integrand, since it results from processes on the cyclotron time scale while the rest of the integrand only changes as a result of variations on the bounce time scale), performing the bounce integral at least guarantees a correct order of magnitude. A special treatment near the turning points is, however, necessary even if the integrand is globally sufficiently well sampled.

4.3. Practical formulae and reduction to known results

In this section, we first establish the relation between our expression for the dielectric response (26) and some found elsewhere in the literature. We assume that $m_g \neq 0$, that the transformation (25*b*) is justified, and that the mode numbers m and m' are close to one another. Explicit formulae for W and the RF diffusion operator are provided.

https://doi.org/10.1017/S0022377898007016 Published online by Cambridge University Press

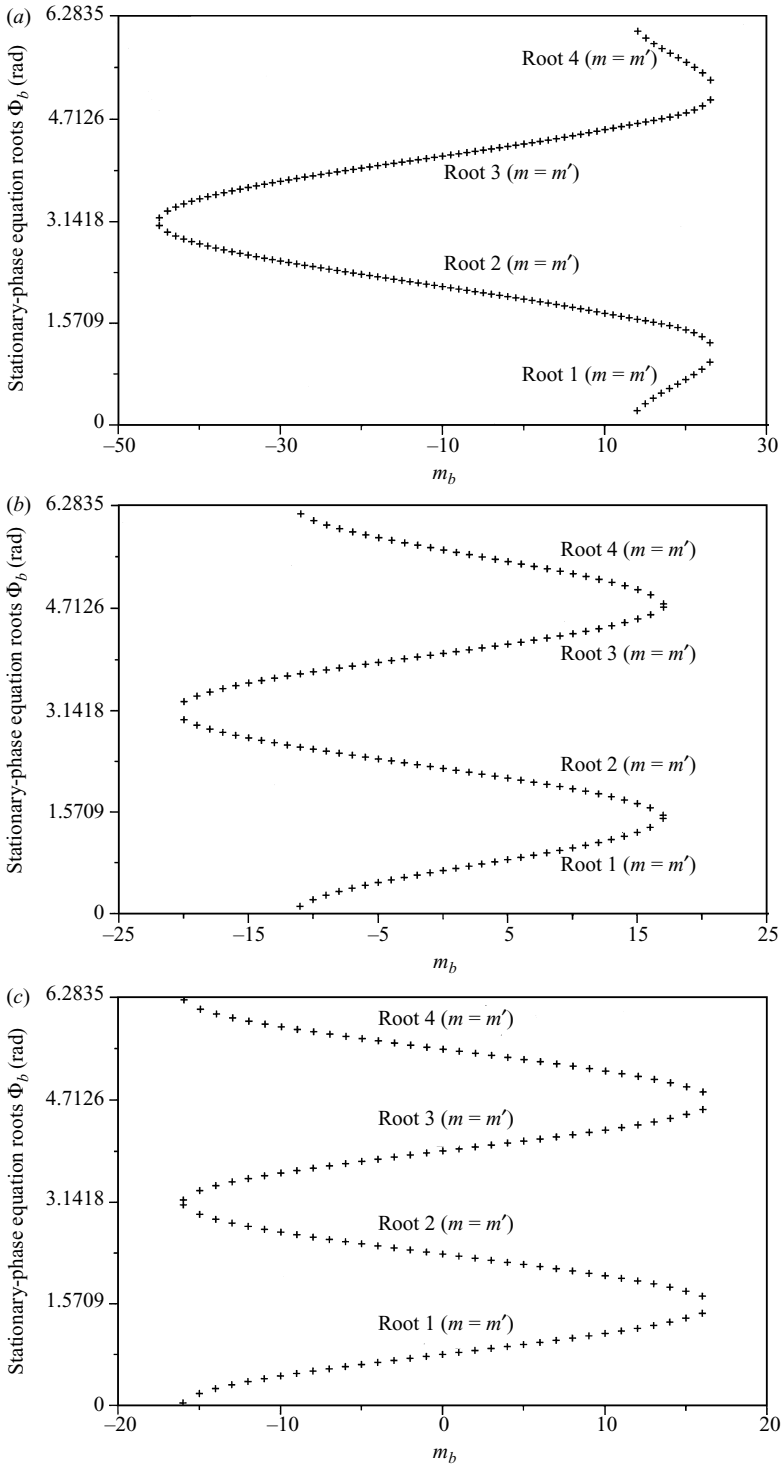


Figure 7. Stationary-phase positions for a deeply trapped H at $r_{gc} = 1.2$ m, with parameters as in Fig. 6, except as follows: (*a*) $m = m' = 10$ and $n = 40$; (*b*) $m = m' = 10$ and $n = 0$; (*c*) $m = m' = n = 0$.

https://doi.org/10.1017/S0022377898007016 Published online by Cambridge University Press

If an analytical expression for Φ_{b_m} in terms of $\Phi_{b_{m'}}$ existed then the dielectric response could be expressed directly as a bounce average without actually having to first compute the bounce spectrum. As was shown in the previous subsection, the bounce spectrum contains a lot of terms for some classes of particles. For these particles, the substitution (25*b*) is most justified, and, just because of the largeness of the bounce spectrum, avoiding having to compute the partial dielectric response for every bounce mode would allow one to significantly speed up numerical evaluation. The relation between the m and m' stationary-phase angles for an identical m_b can be deduced from the stationary-phase condition (19), which can be expressed in the form

$$\Phi_{b_{m'}}(\Phi_{b_m}) = \Phi_{b_{m'}}(0) + \int_0^{\Phi_{b_m}} d\Phi_{b_m} \frac{\Theta''_m}{\Theta''_{m'}}, \tag{30}$$

the integrand in which is not trivially 1, since Θ''_m is to be evaluated at Φ_{b_m} and for poloidal mode number m, while $\Theta''_{m'}$ is evaluated at $\Phi_{b_{m'}}$ using the poloidal mode m'. Finding an analytical expression for $\Phi_{b_{m'}}$ (Φ_{b_m}) without making further simplifications is thus not straightforward. Sacrificing part of the fine structure of the actual dielectric response, an elegant solution was suggested by Lamalle (1994, 1997). Assuming that m is close to m' allows one to replace both m and m' by their average $M = \frac{1}{2}(m+m')$ in the rapidly varying phase Θ in (26) while adding an extra (supposedly slowly varying) factor $\exp[\frac{1}{2}i(m-m')\theta]$ to the slowly varying function $\mathcal{G}$ in (15), i.e. adding a factor $\tilde{\Theta}_{m,m'} = (m-m')\theta$ to the relative phase of the product of the field and the test function. This seems a reasonable assumption, since the cyclotron term causes the most rapid variation of the phase, and the poloidal contribution is a small correction. It can easily be shown analytically that this is indeed a rigorous procedure when the stationary-phase points of the three poloidal mode numbers m, m' and M are sufficiently close. In that particular case, the differences $\Phi_{b_m} - \Phi_{b_M}$ and $\Phi_{b_{m'}} - \Phi_{b_M}$ can be expressed in terms of quantities evaluated at Φ_{b_M} using a Taylor series expansion truncated at second-order terms. One finds

$$\Phi_{b_m} = \Phi_{b_M} - \frac{m-m'}{2}\frac{\theta'(\Phi_{b_M})}{\Theta''_m(\Phi_{b_M})}, \qquad \Phi_{b_{m'}} = \Phi_{b_M} + \frac{m-m'}{2}\frac{\theta'(\Phi_{b_M})}{\Theta''_{m'}(\Phi_{b_M})}, \tag{31a}$$

which yields the predicted (supposedly slowly varying) relative phase factor

$$\tilde{\Theta}_{m,m'} = (m-m')\,\theta(\Phi_{b_M}), \tag{31b}$$

up to higher-order corrections. The advantage of Lamalle's approach is that the stationary-phase points of m and m' are identical, and thus the actual stationary phase positions for each m_b do not have to be evaluated. The expression (26*b*) now simplifies to

$$\mathcal{N}^{\,m}_{\,m'} = \frac{1}{2\pi}\mathcal{L}_{m_g,m'}(\mathbf{F})^* \left[\frac{\partial F_0}{\partial \varepsilon}\mathcal{L}_{m_g,m}(\mathbf{E}) + \frac{\partial F_0}{\partial \mu}\hat{\mathcal{L}}_{m_g,m}(\mathbf{E})\right] \frac{\exp[i(m-m')\,\theta(\Phi_{b_M})]}{|\Theta''_M(\Phi_{b_M})|}. \tag{31c}$$

https://doi.org/10.1017/S0022377898007016 Published online by Cambridge University Press

The resonance position is Doppler-shifted by the same $k_{\parallel \mathrm{average}} v_\parallel$ for both poloidal mode numbers m and m' instead of the actual $k_\parallel v_\parallel$ relevant to each individual poloidal mode, but $k_{\parallel \mathrm{average}} \approx k_\parallel$, since m is close to m'; a similar approach, but dropping the Doppler-shift effects together, was adopted by Belikov and Kolesnichenko (1982). We stress again that the second derivative of the phase Θ in the denominators of (31*b*) goes through zero at the turning points, and so, just as already mentioned when discussing (25), a more refined description is required near such points. With regard to the computation of the RF-induced derivatives of $\mathbf{\Lambda}$, several authors have studied this situation, and have found that it is sufficient to account for the next term in the Taylor series development of the phase around the turning point (see e.g. Stix 1975; Bécoulet *et al*. 1991; Lamalle 1994, 1997). The resonant denominator is hereby replaced by a function involving the Airy function that stays finite when the two stationary-phase positions cross the turning point. We recall that (25) has large but generally finite contributions for m_b corresponding to stationary-phase points near the turning points, since, for arbitrary $\mathbf{\Lambda}$, the probability that the stationary-phase points actually coincide with the turning points (where (17) goes to infinity because Θ'' vanishes) is small; as can be seen from any of the figures containing the roots of the stationary-phase equation (18), the stationary-phase angles vary rapidly with m_b near such points. Consequently the use of the more refined description involving the Airy function (see (20)) is usually unnecessary in practice.

Since the stationary-phase points of the rapidly varying factors corresponding to the test function $\mathbf{F}$ and the electric field $\mathbf{E}$ can be confused, the stationary-phase position subscript is dropped. Absorbing the factors $\exp(im\theta)$ and $\exp(-im'\theta)$ in $\mathbf{E}$ and $\mathbf{F}^*$ respectively, the dielectric response then simplifies to

$$\mathsf{W} = -2\pi\omega\mu_0\left(\frac{q}{m}\right)^2 \int dr_{gc} \frac{\partial \Psi gc}{\partial r_{gc}} \int d\varepsilon \int d\mu \frac{1}{\omega_b} \sum_n \sum_m \sum_{m'} \int_0^{2\pi} d\Phi_b$$

$$\times \frac{1}{M\dot{\theta}_{gc} + n\dot{}_{gc} + m_g\dot{\phi} - \omega} \mathscr{L}_{m_g,m'}(\mathbf{F})^* \left[\frac{\partial F_0}{\partial \varepsilon} \mathscr{L}_{m_g,m}(\mathbf{E}) + \frac{\partial F_0}{\partial \mu} \hat{\mathscr{L}}_{m_g,m}(\mathbf{E})\right], \quad (32a)$$

in which the factor $|\Theta''_M|$ in the denominator of $\mathscr{N}^{\,m}_{m'}$ has been compensated by the same factor appearing in the transformation (25*b*); $M = \frac{1}{2}(m + m')$. In terms of the usual poloidal angle, this becomes

$$\mathsf{W} = -2\pi\omega\mu_0\left(\frac{q}{m}\right)^2 \int dr_{gc} \frac{\partial \Psi gc}{\partial r_{gc}} \int d\varepsilon \int d\mu \sum_n \sum_m \sum_{m'} \int \frac{d\theta_{gc}}{\dot{\theta}_{gc}}$$

$$\times \frac{1}{M\dot{\theta}_{gc} + n\dot{}_{gc} + m_g\dot{\phi} - \omega} \mathscr{L}_{m_g,m'}(\mathbf{F})^* \left[\frac{\partial F_0}{\partial \varepsilon} \mathscr{L}_{m_g,m}(\mathbf{E}) + \frac{\partial F_0}{\partial \mu} \hat{\mathscr{L}}_{m_g,m}(\mathbf{E})\right], \quad (32b)$$

by virtue of

$$d\Phi_b = \omega_b\, dt \quad (32c)$$

and

$$dt = d\theta_{gc}\left(\frac{d\theta_{gc}}{dt}\right)^{-1} = \frac{d\theta_{gc}}{\dot{\theta}_{gc}}, \quad (32d)$$

https://doi.org/10.1017/S0022377898007016 Published online by Cambridge University Press

or, using Cartesian coordinates $\mathbf{r}_{gc}$ and $\mathbf{v}$,

$$\mathsf{W} = -\omega\mu_0 q^2 \int d\mathbf{r}_{gc} \int d\mathbf{v} \sum_n \sum_m \sum_{m'} \frac{1}{k_{\|M} v_\| - m_g \Omega - \omega} \times \mathscr{L}_{m_g,m'}(\mathbf{F})^* \left[\mathscr{L}_{m_g,m}(\mathbf{E}) \frac{\partial}{\partial \varepsilon} + \check{\mathscr{L}}_{m_g,m}(\mathbf{E}) \frac{\partial}{\partial \mu} \right] F_0. \quad (32e)$$

This expression is formally identical to that for a homogeneous plasma, but the differential operators now operate on the test function and the electric field. Also, the finite poloidal field and the toroidicity are accounted for. The special status of orbits having their resonance at the turning points (exhibited by the presence of Θ'' in the denominator of (26)), has been eliminated by the substitution (25*b*) as explained above. This has an important practical consequence: in the limit $\omega_b \ll \nu \ll \omega$, the efficient heating at tangent resonance points is implicitly embedded in the usual plasma modelling! Although the denominator Θ'' of (26*b*) vanishes at or very close to the turning points for these orbits (indicating that the particles in question absorb wave power very efficiently) the substitution (25*b*) reveals that the stationary-phase angles are then widely spaced, resulting in the fact that, looking at the phenomenon *spatially* rather than in velocity space, no trace of this efficient absorption is left.

All quantities in the above expression are known functions of the chosen set of independent variables. For practical use, the usual wavelength-to-Larmor scale ordering is adopted and the differential operators are truncated. Appendix C contains the explicit forms of the operators when terms up to second-order in the (supposedly small) parameter $k_\perp v_\perp/\Omega$ are retained.

The total power absorbed by all guiding-centre orbits is found by replacing the test-function vector $\mathbf{F}$ by $\mathbf{E}$ in the above expressions. Since in the distributional sense

$$\mathrm{Re}\left\{\frac{c}{i(M\dot{\theta}_{gc} + n\dot{}_{gc} + m_g\dot{\phi} - \omega)}\right\} = \pi\,\mathrm{Re}\{c\}\,\delta(M\dot{\theta}_{gc} + n\dot{}_{gc} + m_g\dot{\phi} - \omega),$$

the absorbed power becomes

$$P_{\mathrm{abs}} = -\sum_n \sum_m \sum_{m'} \frac{\pi q^2}{2} \int d\mathbf{x}_6\, J\, \delta(k_{\|M} v_\| - m_g \Omega - \omega) \times \mathrm{Re}\left\{ \mathscr{L}_{m_g,m'}(\mathbf{E})^* \left[\frac{\partial F_0}{\partial \varepsilon} \mathscr{L}_{m_g,m}(\mathbf{E}) + \frac{\partial F_0}{\partial \mu} \hat{\mathscr{L}}_{m_g,m}(\mathbf{E}) \right] \right\}, \quad (33)$$

in which $\mathbf{x}_6 = (r_{gc}, \varepsilon, \mu, \boldsymbol{\Phi})$ but the gyro- and toroidal-angle integrations trivially give rise to a factor $(2\pi)^2$. The above result has an important numerical consequence: in the limit considered here, the computation of the absorbed power does not require the computation of the dielectric response for the whole bounce spectrum or the evaluation of the complete bounce integral. Only the contribution(s) from the resonant bounce mode or the resonant poloidal position(s) is (are) required! Unlike the computation of the absorbed power or the associated diffusion operator, the evaluation of the reactive part of the dielectric response, needed for studying wave propagation, requires the evaluation of the whole spectrum. The search for the resonant position requires finding the roots of $M\dot{\theta}_{gc} + n\dot{}_{gc} + m_g\dot{\phi} = \omega$, i.e. the roots of the equation for

https://doi.org/10.1017/S0022377898007016 Published online by Cambridge University Press

the stationary-phase angles (21) for the particular bounce mode satisfying $\mathbf{m}\cdot\boldsymbol{\omega}=\omega$. Since the value of the resonant Φ_b is not required, this equation can be solved directly in terms of the usual coordinates. For the particular case of circular magnetic surfaces, the dependence of the toroidal and poloidal components of the parallel wavenumber is known analytically, and one readily finds that the resonance condition can be written as (see e.g. Van Eester *et al.* 1996)

$$(v^2\alpha_2^2-\omega^2)R^3+[v^2(2\alpha_2\alpha_3-\alpha_1\alpha_2^2)-2\omega\alpha_4]R^2 + [v^2(\alpha_3^2-2\alpha_1\alpha_2\alpha_3)-\alpha_4^2]R-v^2\alpha_1\alpha_3^2=0, \quad (34)$$

in which R is the resonant major radius and

$$\alpha_1=\frac{\mu}{\varepsilon}\mathscr{B}, \qquad \alpha_2=\frac{M}{r}\sin\tilde{\alpha}, \qquad \alpha_3=n\cos\tilde{\alpha}, \qquad \alpha_4=m_g R_0\,\Omega(R_0). \quad (35)$$

Since exact expressions exist for the roots of a cubic equation, the resonance positions can be found analytically (Abramowitz and Stegun 1972).

Starting from (11) and performing the same algebra, the RF diffusion operator corresponding to the above expressions for the dielectric response and the absorbed power is found to be

$$\begin{aligned}\mathsf{D}&=\frac{1}{J}\begin{pmatrix}\frac{\partial}{\partial\varepsilon} & \frac{\partial}{\partial\mu}\end{pmatrix}J\sum_n\sum_m\sum_{m'}\frac{q^2}{2}\int d\Phi_b\,\delta(k_{\parallel M}v_\parallel-m_g\Omega-\omega)\\ &\quad\times\frac{1}{2}\mathrm{Re}\left\{\begin{pmatrix}\mathscr{L}_{m_g m'}(\mathbf{E})^*\mathscr{L}_{m_g m}(\mathbf{E}) & \mathscr{L}_{m_g m'}(\mathbf{E})^*\hat{\mathscr{L}}_{m_g m}(\mathbf{E})\\ \hat{\mathscr{L}}_{m_g m'}(\mathbf{E})^*\mathscr{L}_{m_g m}(\mathbf{E}) & \hat{\mathscr{L}}_{m_g m'}(\mathbf{E})^*\hat{\mathscr{L}}_{m_g m}(\mathbf{E})\end{pmatrix}\right\}\begin{pmatrix}\frac{\partial}{\partial\varepsilon}\\ \frac{\partial}{\partial\mu}\end{pmatrix}.\\ &=\frac{1}{J}\begin{pmatrix}\frac{\partial}{\partial\varepsilon} & \frac{\partial}{\partial\mu}\end{pmatrix}J\sum_n\sum_m\sum_{m'}\sum_{\mathrm{res}}\frac{q^2}{2}\frac{1}{\frac{d}{d\Phi_b}(k_{\parallel M}v_\parallel-m_g\Omega-\omega)}\\ &\quad\times\frac{1}{2}\mathrm{Re}\{\mathscr{L}_{m_g m'}(\mathbf{E})^*\mathscr{L}_{m_g m}(\mathbf{E})\}\begin{pmatrix}1 & -H_{m_g}\\ -H_{m_g} & H_{m_g}^2\end{pmatrix}\begin{pmatrix}\frac{\partial}{\partial\varepsilon}\\ \frac{\partial}{\partial\varepsilon}\\ \frac{\partial}{\partial\mu}\end{pmatrix}. \end{aligned} \quad (36)$$

The verification of (8f) is immediate. Adopting the time t spent in reaching a poloidal position along the guiding-centre orbit as independent variable, and using

$$\begin{aligned}\delta(M\dot{\theta}_{gc}+n\dot{}_{gc}+m_g\dot{\phi}-\omega)&=\frac{\delta(t-t_{\mathrm{res}})}{|M\ddot{\theta}_{gc}+n\ddot{}_{gc}+m_g\ddot{\phi}|}\\ &\approx\frac{\delta(t-t_{\mathrm{res}})}{\left|m_g\frac{\Omega}{R_{gc}}\sin\theta_{gc}\sin\tilde{\alpha}\,v_\parallel\right|},\end{aligned}$$

leads to a result equivalent to that in Bernstein and Baxter (1981). We recall that $\Phi_b=\omega_b t$, and so performing the integration on Φ_b is equivalent to the usual temporal bounce average. The obtained diffusion operator is thus the

https://doi.org/10.1017/S0022377898007016 Published online by Cambridge University Press

generalization of the RF diffusion operator for a uniform magnetic field (Kennel and Engelmann 1966). It is a sum of contributions evaluated at the resonant position(s). When the resonance condition is not satisfied along the orbit, the diffusion operator is zero. The absorbed power can be written as

$$P_{\rm abs} \approx -2\pi^3\left(\frac{q}{m}\right)^2 \int dr_{gc}\mathscr{B}\int d\varepsilon \int d\mu \sum_n \sum_m \sum_{m'} \sum_{\rm res} \frac{R_{gc}}{|m_g\,\Omega \sin\theta_{gc}\, v_\parallel|}$$

$$\times \mathscr{L}_{m_g,m'}(\mathbf{E})^* \left[\mathscr{L}_{m_g,m}(\mathbf{E})\frac{\partial}{\partial\varepsilon} + \hat{\mathscr{L}}_{m_g,m}(\mathbf{E})\frac{\partial}{\partial\mu}\right] F_0$$

$$\approx -2\pi^3\left(\frac{q}{m}\right)^2 \int dr_{gc}\mathscr{B}\int d\varepsilon \int d\mu \sum_n \sum_m \sum_{m'} \sum_{\rm res} \frac{R_{gc}}{|m_g\,\Omega \sin\theta_{gc}\, v_\parallel|}$$

$$\times \mathscr{L}_{m_g,m'}(\mathbf{E})^* \mathscr{L}_{m_g,m}(\mathbf{E}) \left(\frac{\partial F_0}{\partial\varepsilon} - H_{m_g}\frac{\partial F_0}{\partial\mu}\right),$$

which is the generalization of the bounce-averaged formula proposed by Stix (1975). As mentioned before, orbits for which the resonance occurs close to the midplane or a turning point absorb the wave power efficiently. A small change in energy ε or magnetic moment μ suffices to move the resonant angle θ_{gc} away from the equatorial, since $\partial\theta_{gc}/\partial\varepsilon \propto 1/(v_\parallel \sin\theta_{gc})$. As a consequence, the total amount of power absorbed in the region near the midplane is not particularly abundant unless the distribution function F_0 itself is peaked in the regions of velocity space corresponding to tangent resonance points.

To evaluate the velocity-space integrals, it is necessary to provide the actual distribution function, which is a function of the constants of motion only. Up to this point, the slowly varying distribution function has not been specified and the expressions for the absorbed power and the RF diffusion operator are self-consistent. Using the expression (32*e*) for the dielectric response, one can write the wave equation in the variational form (7) for a general equilibrium (for details, see Lamalle 1997). Practically useful expressions for the particular case of a Maxwellian F_0 are listed in Appendix C.

We recall that the formulae obtained in this section are only trustworthy if the poloidal mode numbers of the field and the test functions are not too far apart. The philosophy behind this procedure is that, although the poloidal modes are not truly decoupled in a tokamak, the cyclotron variation is so fast with respect to the bounce motion that it obscures to some extent the presence of the latter in the evaluation of the bounce spectrum. The poloidal motion then merely gives rise to a supplementary, supposedly slowly varying, factor in the integrand. Obtaining more general analytical results is not straightforward, since the relative position of the saddle points for differing poloidal mode numbers but identical m_b, given formally by (30) and discussed numerically in Sec. 4.3, are not known in closed analytical form. At the price of a substantial amount of CPU time to find the actual saddle-point positions for a given bounce mode, the dielectric response can be evaluated directly from the expression (22). Unlike the approximate expressions, these general expressions do not become singular at the turning points. On the other hand, their relation to well-known uniform plasma results is obscured. The differential operators

https://doi.org/10.1017/S0022377898007016 Published online by Cambridge University Press

in the radial direction remain unchanged, and can be taken from (14) or (C 1) (see Appendix C).

5. Conclusions

Starting from a more general formalism due to Lamalle (1997), the dielectric response and, more particularly, the associated RF diffusion tensor in toroidal geometry have been derived and discussed using a simple decorrelation approach that consists in the addition of a small, positive imaginary part to the driver frequency: $\omega \rightarrow \omega + i\nu$. This amounts to adding an attenuation factor $e^{\nu t}$ to the Vlasov equation. The toroidal geometry and the poloidal magnetic field have been accounted for, but finite-banana-width effects have been neglected. Analytical expressions have been obtained for magnetic surfaces with circular cross-section. The model presented here, the basic ideas of which were sketched in Van Eester (1995), relies on the more general (though formal) pioneering work of Kaufman (1972) on RF heating in toroidal geometry, but yields more practical expressions that reveal a close connection to known results. The adopted independent variables are three constants of the unperturbed motion (energy, magnetic moment, and radial position of the guiding centre) and a set of three angles that vary linearly with time. The choice of the constants of motion as three of the independent variables has the advantage that the plasma contribution to the wave operator appearing in the variational form of the wave equation is directly related to the RF diffusion operator to be used in the Fokker–Planck equation. Moreover, the relation to the action-angle Hamiltonian approach (based on specific 'actions' $\mathbf{\Lambda}$ and angles $\mathbf{\Phi}$ that equally vary linearly with time) is immediate. A self-consistent wave/Fokker–Planck system results; in this paper, the accent has mostly been on the discussion of aspects related to the Fokker–Planck part. As the particle position is not a constant of the motion, the tedious computation of the dielectric tensor is avoided, but knowledge of local quantities at the particle position is sacrificed.

The most painstaking step in the evaluation of the dielectric response in toroidal geometry is the evaluation of the bounce spectrum of 'elementary building blocks' describing the interaction of the individual orbits with the RF wave. In this paper, these building blocks have been found by first evaluating the bounce spectrum of the particle motion, and subsequently evaluating the bounce spectrum of the (much more rapidly varying) elementary contributions themselves using a method proposed in Van Eester (1995). The first step in the process amounts to performing a coordinate change to the angles of the Hamiltonian formalism. The second step amounts to the evaluation of the time-history integral along unperturbed orbits. As is well known by authors adopting the Hamiltonian approach, first performing the coordinate transformation makes this second step trivial.

The global substitution of the continuous bounce integral for the discrete sum on the bounce spectrum modes in the expressions for the dielectric response, the absorbed power and the RF diffusion tensor in toroidal geometry with closed poloidal projections of the guiding-centre orbits has been discussed. Whereas in straight-magnetic-field-line models, the absorbed power is insensitive to the actual value of the decorrelation time as long as the decorrelation is sufficiently weak (i.e. ν is sufficiently small), a lower bound has to be imposed on ν to allow

https://doi.org/10.1017/S0022377898007016 Published online by Cambridge University Press

the substitution of the bounce spectrum by a bounce integral in toroidal geometry. In the case where the substitution is justified ($\omega_b \ll \nu \ll \omega$), poloidally localized resonance points along the orbit appear, and the resulting expressions are closely related to those obtained using quasi-uniform straight-magnetic-field-line plasma models. In the case where $\nu \ll \omega_b \ll \omega$, one is in the superadiabatic regime and global resonances appear. In this regime, as opposed to what is predicted by models relying on a simplified geometry, the absorbed power drops to zero for sufficiently weak decorrelation. Within the limitations of the adopted decorrelation model, the formalism presented here allows one to describe both regimes. The former regime ($\omega_b \ll \nu \ll \omega$) has the advantage that it allows one to proceed further analytically. The latter regime ($\nu \ll \omega_b \ll \omega$) and the transition regime between these two necessitates evaluating the full bounce spectrum, and relies heavily on the details of the individual bounce-spectrum modes.

The bounce spectrum has been investigated for the case of cyclotron interaction. It has been found that the sum of the partial dielectric responses of the bounce spectrum can be substituted locally for a bounce integral over the part of the poloidal circumference that is accessible to the orbit when the bounce spectrum is large. For very energetic particles, deeply trapped particles or particles close to the magnetic axis, however, the conditions under which this substitution is valid are not trivially satisfied and depend critically on the sensitivity of the partial dielectric response for a given bounce mode to the bounce mode number m_b. Moreover, well-separated poloidal modes give rise to displaced spectra, so that part of the bounce integral is to be excluded when evaluating the dielectric response. Near turning points, the validity of this substitution is least well verified. Even when the substitution is globally well justified, it is questionable in the part of the bounce spectrum for which the associated stationary-phase points lie close to the turning points along the orbit. This has the interesting practical consequence that no refined model is required to describe the absorption close to the tangent resonance points, since the probability of having coinciding stationary-phase points *at* the turning points is very small; if such a coincidence occurs, more refined expressions are available in the literature to describe the wave–particle interaction. Another interesting consequence is that the efficient absorption at the tangent resonance points in the constants-of-motion space is not inconsistent with the fact that *spatially* no enhanced heating is observed near the midplane turning points along the orbits.

By representing all expressions in terms of the angles of the Hamiltonian formalism, the results in this paper can be compared directly with those obtained via the Hamiltonian approach. Being based on a general formalism but relying on a simplified wave–particle decorrelation function, and retaining terms up to leading order in the drift parameter only, the (at first glance obscured) close relation between various forms of the RF response and diffusion operators obtained earlier in the literature using more involved (see e.g. Kaufman 1972) or straight-magnetic-field-line models (see e.g. Stix 1975) is shown. The link with the Hamiltonian formalism is immediate: up to a multiplicative factor, the 'elementary building blocks' are the partial perturbed Hamiltonians of individual bounce modes. Deviations from models assuming straight magnetic field lines include extra effects such as poloidal coupling and

https://doi.org/10.1017/S0022377898007016 Published online by Cambridge University Press

tangent resonance heating. Formally, both the usual bounce-averaged RF diffusion operator and the (Maxwellian plasma) expression for the dielectric response involving the plasma dispersion function are recaptured when the cyclotron gyration dominates the poloidal coupling. As mentioned above, the assumptions underlying these simplified models are, however, not trivially satisfied when the toroidal geometry is rigorously accounted for. In that case, the total dielectric response can be found as the sum of the bounce integral in the regions excluding the tangent resonance points, and the sum of contributions corresponding to the bounce-spectrum modes with stationary-phase angles near the turning points.

Acknowledgements

This work has benefited from various discussions with Drs R. Koch and P. U. Lamalle.

Appendix A. Analytical expression for Φ_b for circular magnetic surfaces

The factor $\partial\Psi_{gc}/\partial r_{gc}$ in (1) can most easily be expressed using the relation between the variable Ψ and the poloidal magnetic field:

$$B_p = \frac{1}{2\pi}\left|\frac{\partial \mathbf{x}}{\partial \theta}\right| \boldsymbol{\nabla}\Psi\cdot\boldsymbol{\nabla}\theta\times\boldsymbol{\nabla} \quad ,$$

which for a circular plasma reduces to

$$B_p = \frac{1}{2\pi R}\frac{\partial \Psi}{\partial r},$$

and so

$$\frac{\partial \Psi_{gc}}{\partial r_{gc}} = 2\pi\mathscr{B}\sin\tilde{\alpha},$$

in which $\tilde{\alpha}$ is the angle between the total static magnetic field $\mathbf{B_0}$ and the toroidal direction, and $\mathscr{B} = R_{gc}B_0(R_{gc})$ is a function of r_{gc} only, since both B_p and B_t are inversely proportional to the major radius. Up to terms of order $(B_p/B_t)^2$, it can be approximated by the constant $\mathscr{B} \approx R_0 B_t(R_0)$.

For a circular cross-section, an analytical formula exists for the transit frequency ω_b. For passing particles $(2\tilde{\varepsilon})/(1+\tilde{\varepsilon}) \leqslant \xi_m^2 \leqslant 1)$, the time that a guiding-centre needs to reach a given poloidal position θ along the guiding-centre orbit is

$$t(\theta) = \frac{2r_{gc}}{|\sin\tilde{\alpha}|v}\left[\frac{1+\tilde{\varepsilon}}{(1-\tilde{\varepsilon})\,\xi_m^2}\right]^{1/2}\Pi(\ _{\rm pa}, \nu_{\rm pa}, k_{\rm pa}),$$

while for trapped particles $(0 \leqslant \xi_m^2 \leqslant 2\tilde{\varepsilon}/(1+\tilde{\varepsilon}))$,

$$t(\theta) = \frac{2r_{gc}}{|\sin\tilde{\alpha}|v}\left[\frac{1+\tilde{\varepsilon}}{2\tilde{\varepsilon}(1-\xi_m^2)}\right]^{1/2}\Pi(\ _{\rm tr}, \nu_{\rm tr}, k_{\rm tr}),$$

https://doi.org/10.1017/S0022377898007016 Published online by Cambridge University Press

as can be verified using $\cos\theta$ as the independent variable in various integrals given in Prudnikov *et al.* (1986). In the above, $\tilde{\alpha}$ is the angle between the parallel ($\mathbf{e}_\parallel = \mathbf{B}_0/B_0$) and the toroidal ($\mathbf{e}$) directions, $\tilde{\varepsilon} = r_{gc}/R_0$, ξ_m is $v_\parallel/v$ evaluated in the midplane at the outboard side of the magnetic surface (i.e. at $R_{gc} = R_0 + r_{gc}$), Π is the incomplete elliptic integral of the third kind,

$$\nu_{\rm pa} = \frac{2\tilde{\varepsilon}}{\tilde{\varepsilon}-1}, \quad \nu_{\rm tr} = \frac{1}{1-1/\xi_m^2}, \quad k_{\rm pa}^2 = \frac{1}{k_{\rm tr}^2} = \frac{\nu_{\rm pa}}{\nu_{\rm tr}},$$

$\mathbf{B}_0$ is the static magnetic field, R is the distance from the tokamak's symmetry axis, and R_0 is the major radius. The above formulae are valid for arbitrary aspect ratio, and the angles $_{\rm pa}$ and $_{\rm tr}$ are given by

$$_{\rm pa} = \arcsin\left\{\left[\frac{(1-\cos\theta)\,(R_0/r-1)}{2(R_0/r+\cos\theta)}\right]^{1/2}\right\}$$

$$_{\rm tr} = \arcsin\left\{\left[\frac{(1-\cos\theta)\,(R_0/r+\cos\theta_{\rm max})}{(1-\cos\theta_{\rm max})\,(R_0/r+\cos\theta)}\right]^{1/2}\right\}.$$

In a full bounce, trapped particles pass twice through each poloidal position in the interval $[-\theta_{\rm max}, \theta_{\rm max}]$, and thus the transformation $\theta \to t$ is not single-valued. A 1-to-1 correspondence can be guaranteed by treating the trapped-particle trajectories as being the sum of two passing particles for which part of the poloidal circumference is excluded. Filling in $\theta = \pi$ for passing or $\theta = \theta_{\rm max}$ for trapped particles in the above provides formulae for half the transit time:

$$t_{\rm transit} = \frac{4r_{gc}}{|\sin\tilde{\alpha}|v}\left[\frac{1+\tilde{\varepsilon}}{(1-\tilde{\varepsilon})\xi_m^2}\right]^{1/2} \Pi(\tfrac{1}{2}\pi, \nu_{\rm pa}, k_{\rm pa}) = t_b$$

for passing particles, and

$$t_{\rm transit} = \frac{4r_{gc}}{|\sin\tilde{\alpha}|v}\left[\frac{1\text{-}\tilde{\varepsilon}}{2\tilde{\varepsilon}(1-\xi_m^2)}\right]^{1/2} \Pi(\tfrac{1}{2}\pi, \nu_{\rm tr}, k_{\rm tr}) = \tfrac{1}{2}t_b$$

for trapped particles. The transit time is the bounce time $t_b = 2\pi/\omega_b$ for the passing particles and half the bounce time for the trapped particles. Using the above explicit expressions for the transit time $t_{\rm transit}$ and for the time $t(\theta)$, one readily obtains an analytical expression for $\Phi_b = \omega_b\, t(\theta)$.

Appendix B. The RF-induced time derivatives of ε and μ as a function of (Λ, Φ)

Introducing a rotating frame, characterized by the complex projection vectors $\mathbf{e}_\pm = \frac{1}{2}(\mathbf{e}_{\perp 1} \pm i\mathbf{e}_{\perp 2})$, the components of a vector $\mathbf{w} = w_{\perp 1}\mathbf{e}_{\perp 1} + w_{\perp 2}\mathbf{e}_{\perp 2} + w_\perp \mathbf{e}_\perp = w_+\mathbf{e}_- + w_-\mathbf{e}_+ + w_\parallel \mathbf{e}_\parallel$ are

$$w_\pm = w_{\perp 1} \pm i w_{\perp 2}, \qquad w_{\perp 1} = \frac{w_+ + w_-}{2}, \qquad w_{\perp 2} = \frac{w_+ - w_-}{2i}.$$

https://doi.org/10.1017/S0022377898007016 Published online by Cambridge University Press

In terms of the rotating components, the scalar product of two vectors $\mathbf{w}$ and $\mathbf{v}$ is then

$$\mathbf{w}\cdot\mathbf{v} = \tfrac{1}{2}(w_+ v_- + w_- v_+) + v_\parallel w_\parallel,$$

while the scalar product of the complex conjugate of a vector with another vector is

$$\mathbf{w}^*\cdot\mathbf{v} = \tfrac{1}{2}(w_+^* v_+ + w_-^* v_-) + w_\parallel^* v_\parallel.$$

The scalar product $\mathbf{H}\cdot\mathbf{v}$ is then of the form

$$\mathbf{H}\cdot\mathbf{v} = \mathbf{H}\cdot\mathbf{v}_\perp + v_\parallel H_\parallel = \tfrac{1}{2}v_\perp (e^{i\phi} H_- + e^{-i\phi} H_+) + v_\parallel H_\parallel.$$

The Fourier amplitude of any perturbed quantity $\mathbf{H}(\mathbf{r},t) = \mathbf{H}(r,\theta,\ \ ,t)$, where θ and $\ \ $ are the poloidal and toroidal angles respectively, is of the general form

$$\mathbf{H}(\mathbf{r},t) = \sum_m \sum_n \int dk_r\, \mathbf{H}_\mathbf{k} \exp[i(\mathbf{k}\cdot\mathbf{r} - \omega t)]$$

$$= \sum_m \sum_n \int dk_r\, \mathbf{H}_\mathbf{k} \exp[i(\mathbf{k}\cdot\mathbf{r}_{gc} - \omega t)] \exp\left[-i\frac{v_\perp k_\perp}{\Omega}\sin(\phi-\psi)\right],$$

where

$$k_{\perp 1} = k_r = k_\perp \cos\psi,$$

$$k_{\perp 2} = \frac{m}{r}\cos\tilde{\alpha} - \frac{n}{R}\sin\tilde{\alpha} = k_\perp \sin\psi,$$

$$k_\parallel = \frac{n}{R}\cos\tilde{\alpha} + \frac{m}{r}\sin\tilde{\alpha},$$

and where $\tilde{\alpha}$ is the angle between the static magnetic field and its toroidal component. The last exponential is commonly rewritten using

$$\exp[i\zeta\sin\beta] = \sum_{N=-\infty}^{\infty} \exp(iN\beta)\, J_N(\zeta) \tag{B 1}$$

to make the sum over the cyclotron harmonic spectrum (with terms proportional to $\exp(-iN\phi)$, in which N is the cyclotron harmonic number) explicit. At a given *fixed* time t, $\mathbf{k}\cdot\mathbf{r}$ can be expressed in terms of the set $(\mathbf{\Lambda},\mathbf{\Phi})$ using the following expressions for the guiding-centre motion and the gyrophase evolution (Van Eester 1995):

$$\theta_{gc}(\Phi_b,\varepsilon,\mu,r_{gc}) = \int_0^{\Phi_b/\omega_b} dt\, \mathbf{v}_{gc}\cdot\boldsymbol{\nabla}\theta_{gc},$$

$$_{gc}(\Phi_d,\Phi_b,\varepsilon,\mu,r_{gc}) = \Phi_d + \int_0^{\Phi_b/\omega_b} dt\, \mathbf{v}_{gc}\cdot\boldsymbol{\nabla}\ \ _{gc} - \frac{\omega_d}{\omega_b}\Phi_b$$

$$\phi(\Phi_g,\Phi_b,\varepsilon,\mu,r_{gc}) = \Phi_g + \int_0^{\Phi_b/\omega_b} dt\, \Omega_g - \frac{\omega_g}{\omega_b}\Phi_b,$$

https://doi.org/10.1017/S0022377898007016 Published online by Cambridge University Press

which can be integrated to give

$$\theta_{gc}(\Phi_b,\varepsilon,\mu,r_{gc}) = \frac{1}{\omega_b}\int_0^{\Phi_b} d\Phi_b' \sum_{l=0}^{\infty} \mathfrak{P}_l(\varepsilon,\mu,r_{gc})\cos(l\Phi_b')$$

$$= \delta_{tp}\,\Phi_b + \sum_{l=1}^{\infty}\frac{\mathfrak{P}_l}{l\omega_b}\sin(l\Phi_b), \tag{B 2a}$$

$$_{gc}(\Phi_d,\Phi_b,\varepsilon,\mu,r_{gc}) = \Phi_d + \frac{1}{\omega_b}\int_0^{\Phi_b} d\Phi_b' \sum_{l=1}^{\infty} \mathfrak{T}_l(\varepsilon,\mu,r_{gc})\cos(l\Phi_b')$$

$$= \Phi_d + \sum_{l=1}^{\infty}\frac{\mathfrak{T}_l}{l\omega_b}\sin(l\Phi_b), \tag{B 2b}$$

$$\phi(\Phi_g,\Phi_b,\varepsilon,\mu,r_{gc}) = \Phi_g + \frac{1}{\omega_b}\int_0^{\Phi_b} d\Phi_b' \sum_{l=1}^{\infty} \mathfrak{F}_l(\varepsilon,\mu,r_{gc})\cos(l\Phi_{b)}'$$

$$= \Phi_g + \sum_{l=1}^{\infty}\frac{\mathfrak{F}_l}{l\omega_b}\sin(l\Phi_b), \tag{B 2c}$$

when up–down symmetry of the magnetic surfaces is assumed, taking $\Phi_b = 0$ in the outer midplane, denoting by $\mathfrak{P}_l$, $\mathfrak{T}_l$ and $\mathfrak{F}_l$ the Fourier components of $\dot\theta_{gc} = (\sin\tilde\alpha)\,v_\parallel/r$, $\dot{}_{gc} = (\cos\tilde\alpha)\,v_\parallel/R$ and $\dot\phi \approx -\Omega$ respectively, and using the fact that the angles $\mathbf{\Phi}$ vary linearly with time. The constant δ_{tp} is 1 for passing and 0 for trapped particles. The result is

$$\mathbf{H}(r,t) = \sum_m\sum_n\sum_N \int dk_r\,\mathbf{H}_\mathbf{k}\,J_N(\chi)\exp(iN\psi)$$

$$\times\exp\left\{i\left[k_r\,r_{gc} + m\delta_{tp}\,\Phi_b + n\Phi_d - N\Phi_g + \sum_{l=1}^{\infty}\xi_{l,-N,m,n}\sin(l\Phi_b) - \omega t\right]\right\},$$

the argument of the Bessel functions $\chi = (\zeta_1^2+\zeta_2^2)^{1/2}$, with

$$\zeta_1 = \frac{v_\perp\,k_r}{\Omega},$$

$$\zeta_2 = \frac{v_\perp}{\Omega}\left(\frac{m}{r}\cos\tilde\alpha - \frac{n}{R}\sin\tilde\alpha\right),$$

while $\xi_{l,-N,m,n}$ is given by

$$\xi_{l,\text{-}N,m,n} = \frac{m\mathfrak{P}_l + n\mathfrak{T}_l - N\mathfrak{F}_l}{l\omega_b}. \tag{B 2d}$$

Since each ξ is characterized by four mode numbers (m,n,N,l), labelling it using all four of its subscripts does not contribute to clarity! In the text, only the subscripts that matter at that particular point in the discussion are used, and all others are dropped. The Fourier integral at the particle position is expressed

https://doi.org/10.1017/S0022377898007016 Published online by Cambridge University Press

in terms of Fourier integrals at the radial guiding-centre position. These integrals can readily be evaluated by making a Taylor series expansion of the Bessel function. Performing the Fourier integral then amounts to replacing k_r in the Bessel function by $(1/i)\,d/dr_{gc}$, turning J_N into a differential operator acting solely on $\mathbf{H}$ and not on the Larmor radius $\rho = v_\perp/\Omega$. 'Dotting' this expression into $\mathbf{v}$ gives

$$\begin{aligned}\mathbf{H}\cdot\mathbf{v} = \sum_m \sum_n \sum_N J_N(\chi)\exp[i(m\delta_{tp}\Phi_b + n\Phi_d - \omega t + iN\psi)]\\ \times\frac{v_\perp}{2}\Bigg(\exp\left\{i\left[(-N+1)\,\Phi_g + \sum_{l=1}^{\infty}\xi_{l,-N+1}\sin(l\Phi_b)\right]\right\}H_-\\ +\exp\left\{i\left[(-N-1)\,\Phi_g + \sum_{l=1}^{\infty}\xi_{l,-N-1}\sin(l\Phi_b)\right]\right\}H_+\Bigg)\\ + v_\parallel\exp\left\{i\left[-N\Phi_g + \sum_{l=1}^{\infty}\xi_{l,-N}\sin(l\Phi_b)\right]\right\}H_\parallel.\end{aligned}$$

Appendix C. Dielectric response in circular geometry and for Maxwellian F_0

All quantities in (32) are known functions of the chosen set of independent variables. For practical use, the differential operators are truncated, usually at terms of second order in $k_\perp v_\perp/\Omega$. Remembering that the differential operators in $\mathscr{L}_{m_g,m}$ only act on the field quantities and not on the coefficients, they become

$$\left.\begin{aligned}\mathscr{L}_{0,m}(\mathbf{G}) &= \tfrac{1}{2}v_\perp[\mathscr{J}_1(G_-) + \mathscr{J}_{-1}(G_+)] + v_\parallel\mathscr{J}_0(G_\parallel),\\ \mathscr{L}_{-1,m}(\mathbf{G}) &= \tfrac{1}{2}v_\perp[\mathscr{J}_2(G_-) + \mathscr{J}_0(G_+)] + v_\parallel\mathscr{J}_1(G_\parallel),\\ \mathscr{L}_{1,m}(\mathbf{G}) &= \tfrac{1}{2}v_\perp[\mathscr{J}_0(G_-) + \mathscr{J}_{-2}(G_+)] + v_\parallel\mathscr{J}_{-1}(G_\parallel),\\ \mathscr{L}_{-2,m}(\mathbf{G}) &= \tfrac{1}{2}v_\perp\mathscr{J}_1(G_+) + v_\parallel\mathscr{J}_2(G_\parallel),\\ \mathscr{L}_{2,m}(\mathbf{G}) &= \tfrac{1}{2}v_\perp\mathscr{J}_{-1}(G_-) + v_\parallel\mathscr{J}_{-2}(G_\parallel),\\ \mathscr{L}_{-3,m}(\mathbf{G}) &= \tfrac{1}{2}v_\perp\mathscr{J}_2(G_+),\\ \mathscr{L}_{3,m}(\mathbf{G}) &= \tfrac{1}{2}v_\perp\mathscr{J}_{-2}(G_-),\end{aligned}\right\}\qquad(\mathrm{C}\,1a)$$

where

$$\left.\begin{aligned}\mathscr{J}_0 = J_0 &\approx 1 + (\tfrac{1}{2}\rho)^2\Delta_\perp\\ \mathscr{J}_1 = J_1\exp(i\psi) &\approx -\tfrac{1}{2}i\rho\nabla_-,\\ \mathscr{J}_{-1} = J_{-1}\exp(i\psi) &\approx +\tfrac{1}{2}i\rho\nabla_+,\\ \mathscr{J}_2 = J_2\exp(2i\psi) &\approx -\tfrac{1}{2}(\tfrac{1}{2}\rho)^2\nabla_-^2\\ &\approx -\tfrac{1}{2}(\tfrac{1}{2}\rho)^2\left(\frac{d^2}{dr_{gc}^2} - 2k_{\perp 2}\frac{d}{dr_{gc}} + k_{\perp 2}^2\right),\\ \mathscr{J}_{-2} = J_{-2}\exp(-2i\psi) &\approx -\tfrac{1}{2}(\tfrac{1}{2}\rho)^2\nabla_+^2\\ &\approx -\tfrac{1}{2}(\tfrac{1}{2}\rho)^2\left(\frac{d^2}{dr_{gc}^2} + 2k_{\perp 2}\frac{d}{dr_{gc}} + k_{\perp 2}^2\right),\\ \mathscr{J}_L = J_L\exp(\pm iL\psi) &\approx 0 \quad \text{when } L > 2.\end{aligned}\right\}\qquad(\mathrm{C}\,1b)$$

https://doi.org/10.1017/S0022377898007016 Published online by Cambridge University Press

To evaluate the velocity-space integrals, it is necessary to provide the actual distribution function, which is a function of the constants of motion only. Up to this point, the slowly varying distribution function has not been specified, and the expressions for the absorbed power and the RF diffusion operator are self-consistent. Using the expression (32*e*) for the dielectric response, one can write the wave equation in the variational form (7) for a general equilibrium (for details, see Lamalle 1997). At this point, we restrict ourselves to a Maxwellian

$$F_0 = \frac{N(r_{gc})}{(2\pi)^{3/2} v_t^3(r_{gc})} \exp\left[-\frac{\varepsilon}{m v_t^2(r_{gc})}\right],$$

in which ε is the energy, N the density and v_t the thermal velocity (itself related to the temperature T via $m v_t^2 = \kappa T$, with κ the Boltzmann constant). The absorbed power in a toroidal plasma with circular cross-section and in thermodynamic equilibrium is

$$P_{\rm abs} = 2\pi^3 \left(\frac{q}{m}\right)^2 \int dr_{gc} \frac{\mathscr{B} \sin\tilde{\alpha}}{\kappa T} \int d\varepsilon F_0 \int d\mu \sum_n \sum_m \sum_{m'} \sum_{\rm res} \frac{\mathscr{L}_{m_g m'}(\mathbf{E})^* \mathscr{L}_{m_g m}(\mathbf{E})}{|M\ddot{\theta}_{gc} + n\ddot{\psi}_{gc} + m_g \ddot{\phi}|}.$$

Since the integration over the periodic aspects of the particle motion was performed prior to the integration over the constants of the motion, this formula does not provide any information on the power absorbed in a fixed volume. To compute that quantity, the integration over the velocity-space coordinates in (33) has to be performed first. Reintroducing the local values of $v_\perp$ and $v_\parallel$ as independent variables, we find terms of the form

$$I_{ab} = \int dv_\perp v_\perp \int dv_\parallel v_\perp^a v_\parallel^b \frac{\exp(-mv^2)/2\kappa T}{v_\parallel - v_R}$$

(where $v_R = (\omega + m_g \Omega)/k_{\parallel M}$), which, upon defining

$$I_{\perp a} = \int_0^\infty dp\, p^{a+1} e^{-p^2},$$

$$I_{\parallel b} = \int_{-\infty}^\infty dq \frac{q^b e^{-q^2}}{q - \zeta},$$

can be written in terms of the plasma dispersion function Z with argument $\zeta = v_R/(2\kappa T/m)^{1/2}$ using the following recursion scheme, found by performing partial integrations:

$$I_{ab} = \left(\frac{2\kappa T}{m}\right)^{1+(a+b)/2} I_{\perp a} I_{\parallel b},$$

$$I_{\perp_0} = \tfrac{1}{2}, \qquad I_{\perp 1} = \tfrac{1}{4}\pi^{1/2},$$

$$I_{\parallel 0} = \pi^{1/2} Z, \qquad I_{\parallel 1} = \pi^{1/2}(\zeta Z + 1),$$

$$I_{\perp a} = \tfrac{1}{2} a I_{\perp a-2}, \qquad I_{\parallel b} = \zeta I_{\parallel b-1} + \mathscr{K}_b,$$

$$\mathscr{K}_b = \begin{cases} 0 & \text{when } b \text{ is even,} \\ 2I_{\perp b-2} & \text{when } b \text{ is odd,} \end{cases} \qquad \mathscr{K}_1 = \pi^{1/2}.$$

https://doi.org/10.1017/S0022377898007016 Published online by Cambridge University Press

References

Abramowitz, M. and Stegun, I. A. 1972 *Handbook of Mathematical Functions*. Dover, New York.

Balescu, R. 1988 *Transport Processes in Plasmas*. Vol. I: *Classical Transport*. North-Holland, Amsterdam.

Bécoulet, A., Gambier, D. J. and Samain, A. 1991 *Phys. Fluids* **B3**, 137.

Bécoulet, A., Fraboulet, D., Giruzzi, G., Moreau, D., Saoutic, B. and Chinardet, J. 1994 *Phys. Plasmas* **1**, 2908.

Belikov, V. S. & Kolesnichenko, Y. I. 1982 *Plasma Phys.* **24**, 61.

Bernstein, I. B. and Baxter, D. C. 1981 *Phys. Fluids* **24**, 108.

Brambilla, M. 1994 *Phys. Lett.* **188A**, 376.

Carlsson, J., Eriksson, L.-G. and Hellsten, T. 1997 *Nucl. Fusion* **37**, 719.

Catto, P. J., Lashmore-Davies, C. N. and Martin, T. J. 1993 *Phys. Fluids* **B5**, 2909.

Chen, L. and Tsai, S. T. 1983 *Plasma Phys.* **25**, 349.

Eriksson, L.-G. and Helander, P. 1994 *Phys. Plasmas* **1**, 308.

Gambier, D. J. and Samain, A. 1985 *Nucl. Fusion* **25**, 283.

Jaeger, E. F., Batchelor, D. B., Carter, M. D. and Weitzner, H. 1990 *Nucl. Fusion* **30**, 505.

Kasilov, S. V., Pyatak, A. I. and Stepanov, K. N. 1990 *Nucl. Fusion* **30**, 2467.

Kaufman, A. N. 1972 *Phys. Fluids* **15**, 1063.

Kennel, C. F. and Engelmann, F. 1966 *Phys. Fluids* **9**, 2377.

Lamalle, P. U. 1993 *Phys. Lett.* **175A**, 45.

Lamalle, P. U. 1994 Nonlocal theoretical generalization and tridimensional numerical study of the coupling of an ICRH antenna to a tokamak plasma. PhD thesis, Université de Mons; *LPP-ERM/KMS Laboratory Report* 101.

Lamalle, P. U. 1997 *Plasma Phys. Contr. Fusion* **39**, 1409.

Landau, L. D. and Lifshitz, E. M. 1960 *Mechanics*. Pergamon, Oxford.

Louis, Y. 1996 Etude analytique et numérique de la réponse diélectrique non-local d'un plasma de tokamak à une perturbation radiofréquence, tenant compte de la toroidicité et des effects de décorrélation. PhD thesis, Université Libre de Bruxelles; *LPP-ERM/KMS Laboratory Report* 103.

Louis, Y. 1998 Numerical evaluation of the radio-frequency response of a tokamak plasma with general equilibrium. In preparation.

Louis, Y. and Lamalle, P. U. 1996 *ISPP-17: Proceedings of the Joint Varenna–Lausanne International Workshop on Theory of Fusion Plasmas, Varenna, Italy*, p. 499.

Martin, T. and Václavík, J. 1987 *Helv. Physica Acta* **60**, 471.

Prudnikov, A. P., Brychkov, Y. A. and Marichev, O. I. 1986 *Integrals and Series*, Vol. I, p. 75. Gordon and Breach, New York.

Romero, H. and Scharer, J. 1987 *Nucl. Fusion* **27**, 363.

Stix, T. H. 1975 *Nucl. Fusion* **15**, 737.

Tsai, S. T., Van Dam, J. W. and Chen, L. 1984 *Plasma Phys. Contr. Fusion* **26**, 907.

Václavík, J. and Appert, K. 1987 *Plasma Phys. Contr. Fusion* **29**, 257.

Van Eester, D. 1995 *J. Plasma Phys.* **54**, 31.

Van Eester, D. and Koch, R. 1998 *Plasma Phys. Control. Fusion* (accepted for publication).

Van Eester, D., Louis, Y., Lamalle, P. U. and Koch, R. 1996 *Phys. Lett.* **218A**, 70.

https://doi.org/10.1017/S0022377898007016 Published online by Cambridge University Press